Univerzita Karlova v Praze/Charles University in Prague

Přírodovědecká fakulta/Faculty of Science

Studijní program: Molekulární a buněčná biologie, genetika a virologie

Ph.D. study program: Molecular and Cellular Biology, Genetics and Virology

Mgr. Martina Verdánová

Vliv uhlíkových nanostruktur na chování lidských buněk a význam fetálního bovinního séra během buněčné adheze

The Effect of Carbon Nanostructures on Human Cell Behavior and the Role of Fetal Bovine Serum in Cell Adhesion

Dizertační práce/Ph.D. Thesis

Školitel/Supervisor: doc. RNDr. Marie Hubálek Kalbáčová, Ph.D.

Praha/Prague, 2016

Prohlášení:

Prohlašuji, že jsem závěrečnou práci zpracovala samostatně a že jsem uvedla všechny použité informační zdroje a literaturu. Tato práce ani její podstatná část nebyla předložena k získání jiného nebo stejného akademického titulu.

Statement of authorship:

I declare that I prepared the PhD thesis independently and that I stated all the information sources and literature. This work or a substantial portion thereof has not been submitted to obtain another academic degree or equivalent.

V Praze/In Prague Podpis/Signature

Acknowledgements

I would like to express my sincere thanks to my supervisor doc. RNDr. Marie Hubálek Kalbáčová, Ph.D. for her scientific support, intensive help and great patience during my Ph.D. studies. She created a friendly and stimulating atmosphere for my work. I very thank to all friends and colleagues from the Institute of Inherited Metabolic Disorders and also to other colleagues from many of our collaborative institutes. Special thanks belong to my closest colleagues Tonda, Blanka, Pavla and Lucka for their very friendly and kind attitude to me. It was a pleasure to collaborate with all these people.

Finally, I would like to express my gratitude to my family - to my parents for everything they did for me, to my sister Šárka for being close to me all the time. Special thanks belong to my beloved boyfriend Honza for his unlimited love, support, patience and trust.

Abstrakt

Uhlíkové alotropy - grafen (G) a nanokrystalický diamant (NCD) - patří mezi nadějné nanomateriály vynikající výjimečnou kombinací vlastností jako jsou vysoká mechanická pevnost, elektrická a tepelná vodivost, možnost funkcionalizace a velký poměr povrchu k objemu. Z těchto důvodů jsou G and NCD využívány kromě elektroniky také v biomedicínských aplikacích zahrnujících potahování implantátů, dopravu léčiv a genů do buněk a biosenzory.

Za účelem základní charakterizace chování buněk na G a NCD byla studována adheze a proliferace osteoblastů na těchto materiálech, které byly různě upravené. Obecně lze říci, že G a NCD sloužily jako lepší substrát pro kultivaci osteoblastů než kontrolní polystyren speciálně upravený pro kultivaci buněk. Lepší adheze buněk, ale nižší proliferace, byla pozorována na NCD ve srovnání s G. Nejvíce překvapivé bylo zjištění, že hydrofobní G s nanostrukturovaným povrchem výrazně více podporoval proliferaci buněk ve srovnání s hydrofilním a plochým G a s oběma NCD (hydrofobním i hydrofilním), které měly mírně drsnější povrch. Díky zvýšené proliferaci buněk může dojít k rychlejšímu osídlení G a NCD buňkami a díky tomu k rychlejší tvorbě nové tkáně, což je žádoucí v biomedicínských aplikacích.

Dále bylo ukázáno, že adheze osteoblastů byla zvýšena za počáteční nepřítomnosti fetálního bovinního séra (FBS), nicméně proliferace osteoblastů byla za těchto podmínek snížena bez ohledu na použitý materiál. V návaznosti na tento rozdíl byla na třech typech buněk charakterizována buněčná adheze na polystyren pro tkáňové kultury v přítomnosti a nepřítomnosti FBS. Shodně pro všechny testované typy buněk bylo zjištěno, že během adheze buněk v nepřítomnosti FBS nebyly vytvořeny klasické fokální adheze. Také signalizace v těchto buňkách probíhala neobvyklým způsobem. Naopak v různých typech buněk nepřítomnost FBS ovlivnila tvar, plochu a počet buněk různě. Kontakt adherentních buněk se substrátem v nepřítomnosti proteinů ze séra byl poprvé detailně popsán v této práci.

V poslední části dizertace bylo zkoumáno použití sericinu (“hedvábný” protein) jako náhrady za FBS při zmrazování linie osteoblastů a lidských mezenchymálních kmenových buněk (hMSCs). Bylo ukázáno, že 1% sericin může nahradit 25% FBS ve zmrazovacím médiu pro hMSCs na rozdíl od linie osteoblastů. Kromě toho hMSCs mohou být úspěšně zmrazeny také v růstovém médiu obsahujícím pouze 10% dimethylsulfoxid. Závěrem lze říci, že různá složení zmrazovacích médií by měla být zkoumána pro každý typ buněk zvlášť, aby bylo dosaženo co nejlepších výsledků.

Abstract

Graphene (G) and nanocrystalline diamond (NCD) are carbon allotropes and promising nanomaterials with an excellent combination of their properties, such as high mechanical strength, electrical and thermal conductivity, possibility of functionalization and a very high surface area to volume ratio. For these reasons, G and NCD are employed next to electronics in biomedical applications, including implant coating, drug and gene delivery and biosensing.

For a fundamental characterization of cell behavior on G and NCD, we studied osteoblast adhesion and proliferation on differently treated G and NCD. Generally, both G and NCD exhibited better properties for osteoblast cultivation than control tissue culture polystyrene. Better cell adhesion but lower cell proliferation were observed on NCD compared to G. The most surprising finding was that hydrophobic G with nanowrinkled topography enhanced cell proliferation extensively, in comparison to hydrophilic and flat G and both NCDs (hydrophobic and hydrophilic) with slightly higher roughness. Promoted cell proliferation enables faster cell colonization of G and NCD substrates, meaning faster new tissue formation which is beneficial in biomedical applications.

Furthermore, it was shown that osteoblast adhesion was promoted in the initial absence of fetal bovine serum (FBS); however, osteoblast proliferation was suppressed regardless of the material used. As a follow-up to this difference, we characterized cell adhesion to tissue culture polystyrene in the presence and absence of FBS with three different cell types. Consistently for all tested cell types, no classic focal adhesions were formed during cell adhesion in the absence of FBS proteins. Moreover, signaling within these cells proceeded in an unusual manner. In contrast, FBS absence affected cell shape, area and number variously in the tested cell types. For the first time, the cell-substrate contact in the absence of serum proteins for anchorage-dependent cells was described in detail.

In the last part of this thesis, the use of sericin (silk protein) as a replacement for FBS in freezing medium for osteosarcoma cell line and primary human mesenchymal stem cells (hMSCs) was evaluated. It was shown that 1 % sericin could substitute for 25 % FBS in the freezing medium for hMSCs, in contrast to osteosarcoma cell line. Moreover, hMSCs could be cryopreserved in a growth medium containing only 10 % dimethyl sulfoxide with adequate results. Finally, different freezing formulas should be evaluated for different cell types to find the most satisfactory results.

Table of Contents

1 INTRODUCTION

1.1 Carbon nanomaterials

Nanomaterial is defined as a material smaller than 100 nm at least in one dimension. Nanomaterials in general possess unique properties compared to the bulk materials; the greatest advantage of a nanomaterial is the very high surface area to volume ratio (1). Moreover, the nanoscale organization is naturally found in cell environments in the body. Carbon nanomaterials belong among the most investigated, discussed and applied nanomaterials. In particular, carbon nanomaterials include sp^2-bonded materials such as fullerens, graphene and carbon nanotubes and sp^3-bonded nanodiamonds (Fig. 1). The basic unit of sp^2-bonded carbon nanomaterials is one sheet of graphene. The nanotubes are graphene sheets rolled into tubes, and fullerens are graphene sheets folded into ball-like structure. Several superimposed graphene layers form graphite that is often used as a starting material for a production of various types of carbon nanomaterials (2).

The most of carbon nanomaterials exhibit superior properties such as excellent electrical and thermal conductivity, high mechanical strength, great optical properties and possibility of functionalization (3). These features predetermine carbon nanomaterials for use in various applications such as electronics, sensors and biomedicine. In biomedicine, carbon nanomaterials could be used in drug delivery, tissue engineering, bio-sensing and imaging, laboratory and diagnostic techniques (4).

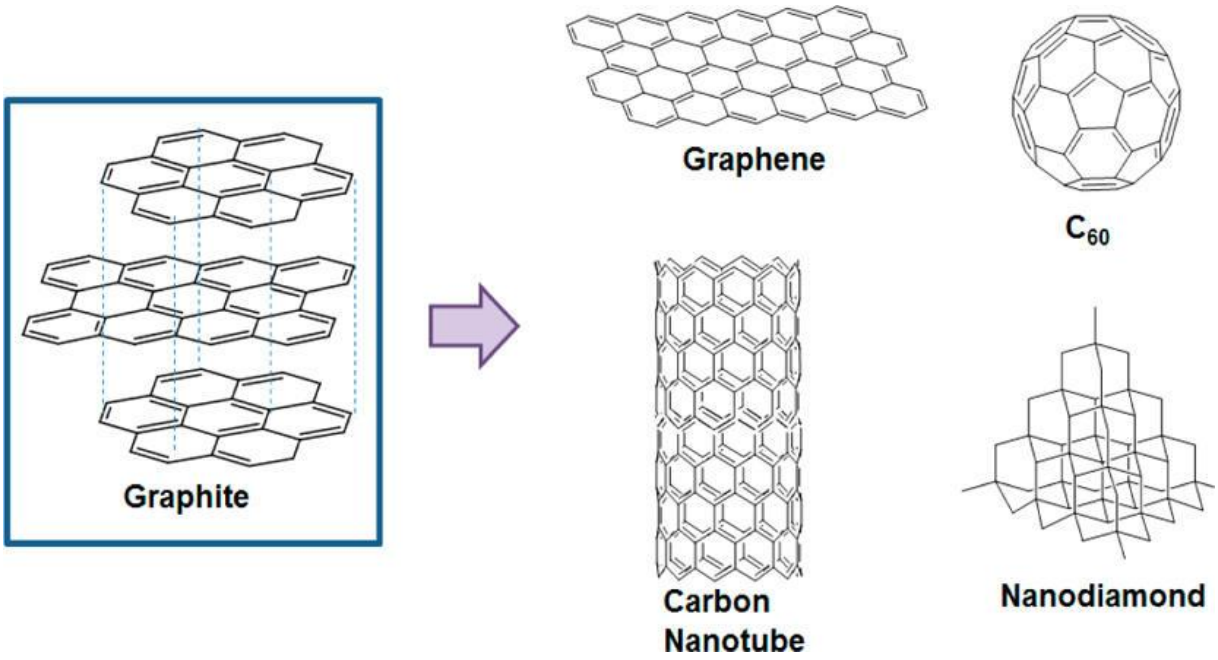

Figure 1: **Various types of carbon namomaterials.** C_{60} = fullerene. Adopted from Cha *et al.*, 2013 (3).

1.1.1 Graphene

Graphene (G) is a single-atom-thick layer of sp^2-bonded carbon atoms arranged in a two-dimensional honeycomb structure. Andre Geim and Konstantin Novoselov were awarded by the Nobel Prize in Physics for "groundbreaking experiments regarding the two-dimensional material graphene" in 2010 (5). G possess various unique properties such as superior electrical and thermal conductivity, extreme mechanical strength, possibility of functionalization, excellent optical transparency and high surface area where every atom is on the surface (4, 6-9).

1.1.1.1 Preparation methods of graphene

Mechanical cleavage from graphite flakes using a Scotch tape, exfoliation of natural graphite flakes using organic solvents or chemical vapor deposition (CVD) are examples of preparation methods of G (10). The widespread method for G production is CVD method which enables a production of large areas of G (up to 150 cm^2) (11). It is a substrate-based method where G is grown on a metal substrate (usually copper) in hydrocarbon gas environment at a high temperature. G prepared by this method has to be transferred from cytotoxic substrate where is usually grown to another material

(often glass or SiO_2/Si) by a special technique based on polymer and its degradation afterwards. By this way, G copies the topography of the new substrate underneath.

1.1.1.2 Types of graphene

The various types of G with different properties could be prepared. Based on number of layers in the graphene sheet, a single layer and a multi-layer G can be distinguished. Based on a preparation method and chemical modifications different types of G could be prepared, e.g. graphene oxide (GO) or reduced graphene oxide (rGO) (12). Hydrophilic GO is easily dispersible in water due to the presence of the oxygen groups. GO is often characterized as an electrical insulator due to the disruption of its sp^2-bonded structure. On the other hand, hydrophobic rGO possesses a great electrical conductivity due to renewal of the G hexagonal lattice. In contrast to GO, rGO has a tendency to create aggregates and therefore it can be dispersing hardly. All Gs can be further functionalized in many ways resulting in changes of G properties (13).

1.1.1.3 Applications of graphene

Besides electronics, G can be used in various biomedical applications including drug and gene delivery, cancer therapy, biosensing, and bioimaging. In addition, G is investigated as an antimicrobial material and as a substrate for cell culture (14).

It was reported that G is able to bind single-stranded DNA specifically and protect it from nucleases which is employed for plasmid DNA delivery to cells (15). GO is often used as a drug carrier thanks to its reactive COOH and OH groups that facilitate attachment of various polymers and biomolecules, e.g. anticancer drugs to GO (16). Further, G could be used as an electrochemical, impedance, electrochemiluminescence or fluorescence biosensor thanks to its electroactivity and transparency (17). As bioimaging agents, graphene quantum dots exhibiting intrinsic fluorescence were prepared (18). An example of antimicrobial activities of G are G nanosheets which can disrupt bacteria membrane and also can induce an oxidative stress and herewith defend against bacteria (19). For these antimicrobial purposes, GO-silver nanocomposites were also tested with promising results (20).

G is widely used as a platform for cell culturing; specifically for tissue engineering and regenerative medicine purposes. It was shown, that G is a biocompatible substrate for human osteoblast and mesenchymal stem cell (MSC)

cultivation (21). Also accelerated osteogenic differentiation of MSCs on G was observed thanks to a G function as a pre-concentration platform for osteogenic inducers. On the other hand, the adipogenic differentiation of MSCs was suppressed on this G (22). Also a special topography of G nanogrids acted as a platform for fast osteogenic differentiation of MSCs (23). Another study described a different behavior of induced pluripotent stem cells (iPSCs) on rGO and GO. The GO substrate promoted adhesion, proliferation and differentiation of iPSCs. However, rGO maintained the iPSCs in the undifferentiated state (24). Coating of various materials by single layer graphene also showed beneficial properties for cultivation of fibroblasts (25).

1.1.1.4 Cytotoxicity of graphene

Cytotoxicity of G is a controversial and widely discussed issue. The already mentioned cytotoxicity for bacterial cells is mostly useful. However, the cytotoxicity for eukaryotic cells (except the cancer cells) is undesirable. The toxicity of G is closely related to its surface functionalization, size and concentration. For example, GO without any functionalization is unstable in a physiological environment and causes cytotoxicity *in vitro* and *in vivo* in dose-dependent manner (26). The comprehensive study of cytotoxicity of GO and rGO revealed a distinct mechanism of a cellular damage. The hydrophilic GO demonstrated cellular uptake, whereas, the hydrophobic rGO mostly adsorbed on a cell surface without internalization. However, the DNA damage and oxidative stress as the cytoxic responses were observed for both GO and rGO but with differential dose dependency (27). The cytotoxicity of G could be significantly decreased by biocompatible coatings (e.g. by polyethylene glycolysation) (28). Therefore, a systematic and long term evaluation of particular G usage has to be performed before a clinical application of this nanomaterial.

1.1.2 Nanocrystalline diamond

Nanocrystalline diamond (NCD) is made up of tetrahedral clusters of sp^3-bonded carbon. NCD exhibits exceptional properties such as high mechanical strength, chemical and corrosion resistance, biocompatibility, excellent optical transparency, possibility of functionalization and extraordinary electrical conductivity (29-31). The most frequently used method for NCD preparation is CVD and its variations (e.g. Hot

Filament CVD, Microwave Plasma CVD or Direct Current Plasma CVD) that enable to produce diamond films over large areas (up to 200 cm^2) (32-35).

NCD surface can be variously modified by chemical, photochemical and electrochemical strategies resulting in various properties of NCD. As grown NCD can be considered as being hydrogen terminated evincing a conductive behavior and a hydrophobic character. Contrary, oxygenated diamond is an electrical insulator with a hydrophilic character. The oxidation of hydrogen terminated diamond can be achieved by thermal, plasma or electrochemical techniques. The oxygen plasma is considered as the most efficient method. NCD surface can be also functionalized by various molecules such as DNA, peptides or proteins (36).

1.1.2.1 Applications of nanocrystalline diamond

Nanodiamond could be used in various applications such as drug and gene delivery (e.g. hybrid nanodiamonds with surface-immobilizated polyethyleneimin for plasmid DNA delivery (37)), cell labeling (e.g. specific cancer cell labeling and tracking by using the fluorescent and magnetic nanodiamond (38)) or biosensing (e.g. diamond films as impedance sensors for a real-time and label-free monitoring of cell growth (39)). Further, NCD is widely used as a substrate for cell culturing for tissue engineering purposes (e.g. use of NCD as a coating of orthopedic implants (40)). Thanks to the possibility of functionalization of NCD, different properties could be achieved and subsequently different cell behavior could be observed. For example, the patterned neuronal growth on variously patterned NCD using photolithography and reactive ion etching was observed (41). Selective osteoblast adhesion on oxygen parts of stripped NCD in comparison to the hydrogen parts was discovered depending on cell seeding density and presence of serum proteins (42). The NCD surface properties (hydrogen or oxygen termination) can affect osteogenic cell differentiation (43) and also the preference of neural stem cells differentiation into distinct cell types (44).

NCD was also investigated for its antimicrobial activity. The antibacterial and bactericide effects of NCD greater than silver but lower than copper were reported (45). Also NCD resistance to bacterial colonization higher than titanium and medical steel was observed (46).

1.1.2.2 Cytotoxicity of nanocrystalline diamond

As mentioned above, NCD can exhibit some antimicrobial properties. However, in contrast to the other carbon based nanomaterials, only mild (47) or no cytotoxicity of NCD films or diamond nanoparticles for eukaryotic cells (e.g. glioblastoma and hepatoma cells, macrophages, keratinocytes, osteoblasts, and fibroblasts) has been reported yet (48-51).

1.2 Material surface properties affecting cell behavior

The cells are able to sense the surrounding environment in multiple length scales. The cell behavior and cell commitment at all are affected by various cues coming from other cells, extracellular matrix (ECM) or artificial materials around them. In this thesis, the focus is on material surface properties and their effect on cell behavior. The knowledge of an interface between cells and materials is essential for a variety of applications. It is important to mention that the proteins from the body fluids or culture medium adsorb on the surface faster than do the cells themselves. Consequently, the cell adhesion is affected by the adsorbed protein layer to a large extent. Therefore, the surface properties of various materials are important primarily for the protein adsorption (the amount and conformation of adsorbed proteins) (52). Surface wettability, topography and charge/energy state of carbon nanomaterials play an important role in modulation of cell behavior. Generally, also substrate stiffness has a significant effect on cell behavior, especially on cell differentiation (53). However, the stiffness of G and NCD themselves (the materials studied in this thesis) is high and dependent of substrate underneath; therefore, a material stiffness will not be further discussed here.

1.2.1 Surface wettability

The cell surface is composed of plenty of proteins, lipids and sugars which dynamically change and the different surface wettability therefore affects the cell behavior largely. The surface wettability is commonly characterized by a water contact angle (CA) measurement. Generally, the material surface is considered as hydrophilic if CA is smaller than approximately 90°. Conversely, the hydrophobic surface reveals CA higher than approximately 90° (54).

Generally, the contradictory results were reported as regards the effect of surface wettability on protein adsorption (protein amount and conformation) and subsequent

cell adhesion, proliferation and differentiation. From this point of view, the most studied proteins are ECM proteins such as fibronectin (FN) or serum proteins such as bovine serum albumin (BSA) or human serum albumin. FN adsorbs preferentially on hydrophilic surfaces resulting in increased cell adhesion; whereas BSA adsorbs predominantly on hydrophobic surfaces resulting in decreased cell adhesion (55). On the other hand, the reports emphasizing the hydrophobic surfaces can be also found, e.g. the higher amount of adsorbed collagen was observed on the hydrophobic surface compared to the hydrophilic one (56). In addition, the hydrophobic surface promoted embryonic stem cells differentiation (57).

Concerning cell behavior on G and NCD, hydrophilic surfaces were favored rather than the hydrophobic ones – e.g. the hydrophilic GO supported cell cultivation and differentiation of iPS cells to higher extent in comparison to the hydrophobic G (58). The favored adhesion of human renal epithelial cells to NCD treated with oxygen (NCD-O) compared to NCD treated with hydrogen (NCD-H) was also reported (59). Similar preference of osteoblasts to NCD-O was observed on NCD with O/H stripes. This preference was guided by the different conformations of proteins from fetal bovine serum on NCD-O and NCD-H (60).

Therefore, the protein and cell response to a surface wettability depends on a particular degree of wettability as well as on a particular protein and cell type and their amount.

1.2.2 Surface topography

The cells are able to sense various cues in their environment in the scale depending on their own size. The micro- and nanoscale milieu is natural for cells. Moreover, the ECM proteins exhibit plentiful nanoscale structures and thus artificial substrates developed for cell culturing try to mimic the native ECM also in nano- and microscale. The surface roughness of various substrates has a significant effect on cell response in general; however, different cell behavior was observed depending on the scale of roughness (micro- vs. nanoscale) (61, 62). NCD with various nanocrystallinity or NCD film deposited on differently rough substrate can be prepared in contrast to G that has a flat surface by itself. However, G can also be transferred to some structured material and hereby can adopt the topography of an underneath substrate (63, 64).

Specifically, the NCD films with nanoroughness [root mean square (RMS) 20 nm] promoted osteoblast adhesion and osteogenic differentiation compared to the flat control polystyrene (65). Another study has suggested that the nanostructures alone may affect proliferation of osteoblasts, while the combination of micro-/submicroscale roughness with a high density of nanoscale structures improves osteoblast differentiation (66). In addition, *in vivo* study with rat tibia has revealed that the screw-shaped implants with high density of nanofeatures (60 nm) induced higher bone formation significantly in comparison to the 120 nm and 220 nm semispherical nanostructures (67).

The distribution of topographical cues is also important for cell behavior. The study of Hart *et al.* revealed that cell adhesion and spreading of human bone marrow cells was reduced on the hexagonal distribution of topographical cues compared to the square distribution (68). In addition, increased osteoblast adhesion and spreading was observed on the substrate with random distribution of nanopits compared to the square distribution (69). Further, the nanoscale disorder promoted MSCs osteodifferentiation even in the absence of osteogenic factors (70).

Since nano- and microtopography plays an important role in guiding cell behavior, various techniques have been developed for a production of biomaterials with controlled topography.

1.2.3 Surface charge and energy state

The surface charge and energy state are related to the surface wettability. Generally, surfaces with high free energy elevated cell adhesion and spreading whereas substrates with low free energy suppressed adhesion and spreading (71). This trend was observed both in the presence and absence of serum proteins on the material surface (72). Moreover, it was demonstrated that surface energy is proportional to cellular adhesion strength (73). As regards surface charge, it was demonstrated that fibroblasts and osteoblasts attached and spread better on the positively charged substrates than on negatively charged ones (74). Similar results were published by Jung *et al.*: as the degree of charge density of substrate increase, the more cell adhesion and proliferation were observed. However, this effect was abolished in the absence of serum (75).

In conclusion, also surface charge and energy state of substrate underneath the cells play a significant role in the adhesion process as well as in a subsequent cell fate

and these characteristics should be taken in consideration when we are thinking about surface properties that affect cell behavior.

1.3 Cell adhesion

Cells receive external signals in form of soluble molecules (cytokines, hormones and growth factors) or by direct interaction with other cells (cell-cell contact) or by contact with the ECM. The information obtained from the cell surrounding is integrated in the cell and affects the cell migration, proliferation, differentiation and death through the cell signaling and changes in gene expression (76). The adhesion of cells to each other and to the ECM is essential for proper cell functions and formation of multicellular structures, tissues and organs. The cell adhesion strongly affects development of organisms, function of immune system, tissue homeostasis, wound repair and also various disorders, especially cancer metastasis. The following text will be focused on the interaction of cells with ECM and environment surrounding the cells. The interaction between the cells and the surrounding ECM is bidirectional, cells sense their environment (outside-in direction) and also cells (specifically cell enzymes) actively remodel the ECM (inside-out direction) (77, 78). The life of anchorage-dependent cells is reliant on the appropriate cell adhesion. If these cells do not receive specific signals for surviving, they die through special cell death called anoikis (a Greek word meaning “loss of home”) (79, 80).

1.3.1 Phases of cell adhesion

The contact of cells with substrates involves several phases during both, *in vitro* and *in vivo* cultivation (Fig. 2). First, the proteins from the body fluids or culture medium adsorb on the surface. Second, the primary contact of cells with the adsorbed protein layer occurs in seconds and comprises of physico-chemical linkage mediated by intermolecular, ionic and van der Waals forces. The third phase takes minutes and involves the cell attachment to the substrate and their little spreading. The cell membrane receptors called integrins bind specific ligands on the surface. Fourth, the clustering of integrin receptors, active cell spreading and reorganization of cytoskeleton occur in hours. The cells engage their acto-myosin cytoskeleton by which sense and also generate the mechanical forces at the sites of adhesion with a subsequent effect on gene expression. The cell shape stability is maintained mostly by the stress of actin

fibres throughout the whole cell. Finally, the cells synthesize their own ECM at their interface with adjacent environment within days (81).

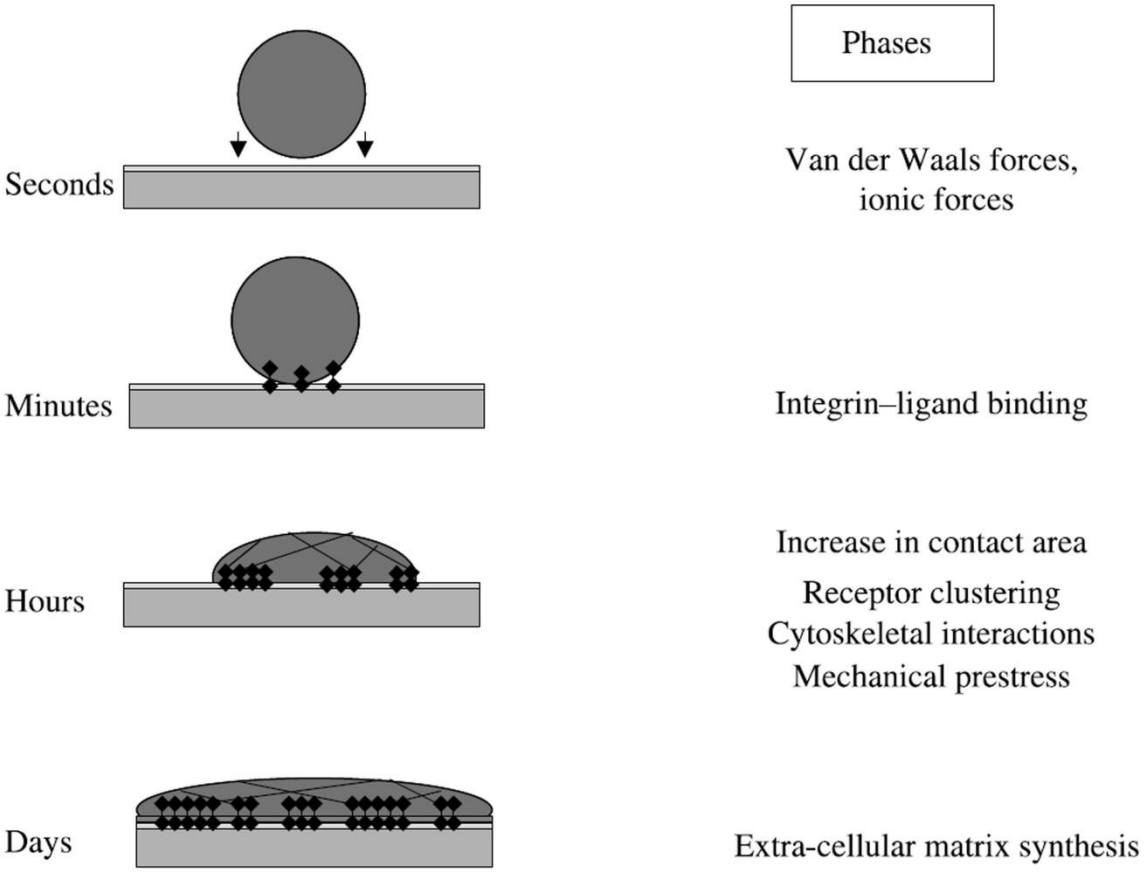

Figure 2: **Phases of cell adhesion process.** Adopted from Anselme *et al.*, 2010 (81).

1.3.2 Integrins

Integrins are the leading proteins of cell adhesion. They are transmembrane heterodimeric receptors binding to various ligands in ECM such as FN, vitronectin (VN), collagen, laminin and many others. Integrins consist of two different chains –α and β subunits. In mammals, the 18 α-subunits and 8 β-subunits join to form 24 different heterodimeric receptors (82). Integrins are sometimes called "promiscuous" because each type of integrin (a specific combination of α and β subunits) can bind more types of ligands and vice versa also one kind of ligand could be bound by several kinds of integrins (83). Every subunit has a large extracellular domain, a single transmembrane helix, and in most cases (except of β4), a short unstructured cytoplasmic domain (84). The conformational changes in integrins that affect their affinity to ligands

could be modulated bidirectionally, by the external ligands and also by the cytoplasmic adaptors. For example, kindlin and talin are such cytoplasmic adaptors which mediate interactions between the integrins bound to proteins in ECM and the actin fibres (85).

Integrins can assume two basic states – inactive with low affinity to the ligand and active with high affinity to the ligand. The intermediate step is so called primed state of integrins with medium affinity to the ligand (86). The switch between the low affinity state and the high affinity state is termed integrin activation. The integrin activation is promoted by the translocation of talin and kindlin to β integrin cytoplasmic tails. This translocation is provoked by integrin-independent signals. The integrin activation enhances the affinity of particular integrins for the particular ECM ligand and thus integrin clustering and formation of focal adhesions (protein complexes linking cell to ECM) can occur (87).

Interestingly, integrins can also cooperate with growth factor receptors. The action of growth factor receptors could be stimulated by integrin clustering and binding of specific ligands. Under these conditions, the transient aggregation of growth factor receptors in the absence of growth factor ligands was observed (88). Moreover, integrins can trigger the same signaling pathways as growth factor receptors. In addition, integrins can directly bind the growth factors or growth factor receptors and arrange their endocytosis and recycling (89).

1.3.3 Focal adhesions

Focal adhesions (FAs) are micron-sized protein assemblies that link the ECM to the actin cytoskeleton in cells to mediate cell adhesion, migration, mechanotransduction and signaling. In the literature, the synonyms for FAs could be found such as focal contacts, focal plaques or focal adhesion sites (90-92). FAs are dynamic complexes which assembled and disassembled while the cell is moving or finds oneself in a new environment. FAs play the two main roles – structural and signaling in the response to cell adhesion on the ECM or another substrate in order to transmit the information from the ECM to the cell nucleus where the changes in gene expression occur.

The FA architecture could be classified into several functional layers (Fig. 3) (93). From the exterior of the cell, the integrin extracellular domain is the first. The second architectural and functional unit of FAs is integrin signaling layer located under the plasma membrane. This layer composes of intracellular part of integrins, protein paxillin, focal adhesion kinase (FAK) and many other proteins that transduce the signal

throughout the cell and herewith regulate the adhesion dynamics and gene expression. The following unit of FAs is the force transduction layer consisting of the proteins that mediate the mechanical linkage between integrins and actin filaments, as talin and vinculin (94). The last part of FAs is the actin regulatory layer composing of e.g. zyxin and vasodilator-stimulated phosphoprotein which are applied in FA strengthening. This layer is followed by actin stress fibres cross-linked by α-actinin (93).

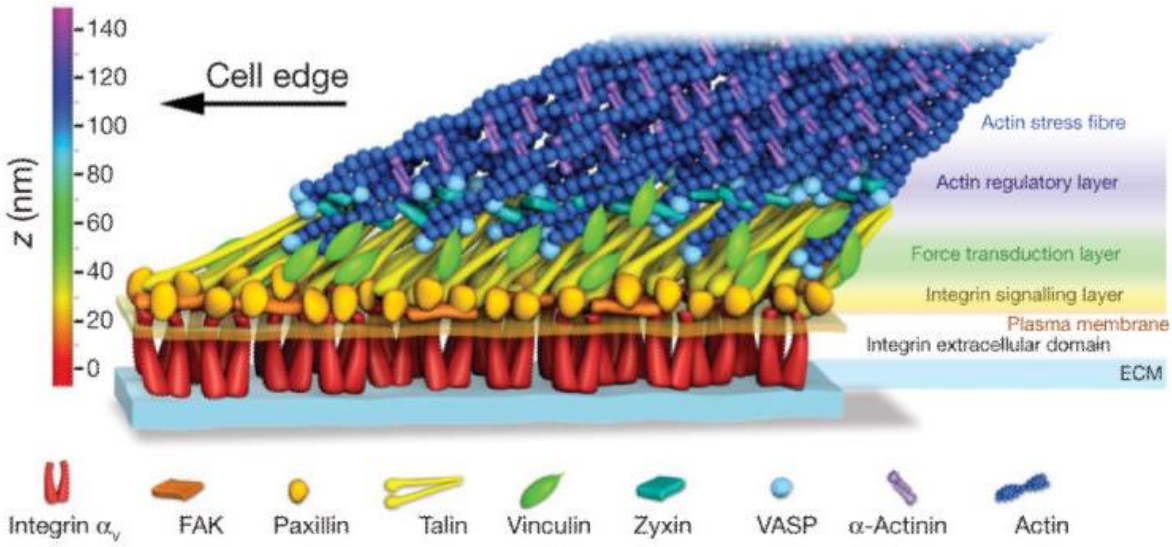

Figure 3: Model of molecular architecture of focal adhesions. Adopted from Kanchanawong *et al.*, 2010 (93).

1.3.3.1 Formation and types of focal adhesions

After integrin clustering, the unstable structures called **nascent adhesions** (or **initial adhesions**; <1 μm^2 in area) are formed in lamellipodia (actin protrusions on the leading edge of the cell) within 60–90 s followed by Rac-dependent maturation to dot-like **focal complexes** which involves recruitment of vinculin (structural cytoskeletal protein) (95). These focal complexes progress to larger **FAs** in Rho-dependent manner. The FAs are the classic and basic units of integrin-mediated cell adhesion that consisted of plenty of proteins and are located mainly in the cell periphery. FAs require approximately 60 minutes to become fully established (96). The most mature adhesions are called **fibrillar adhesions** (or **ECM contacts**), they are elongated structures located close to the cell centre and associated with the ECM fibrils. **Podosomes** are the special type of ECM adhesions. They are small (~ 0.5 μm in diameter) cylindrical structures which can assemble into belt-like superstructures. Podosomes are connected to cellular

motility and invasion (97) and are produced by specialized cells such as invasive cancer cells, osteoclasts, macrophages and dendritic cells. The forms of described adhesions are presented in Fig. 4.

It should be mentioned that F-actin is present at the adhesion site from the beginning and has an active role there. The establishment of FAs is mediated by the activation of Rho, Rac and Cdc-42 proteins which provoked actin polymerization and formation of lamellipodia and filopodia. Lamellipodia are developed at the leading edge of cells and compose of meshwork of branched actin filaments. Filopodia are microspikes often associated with lamellipodia and contained actin filaments cross-linked into the bundles (98).

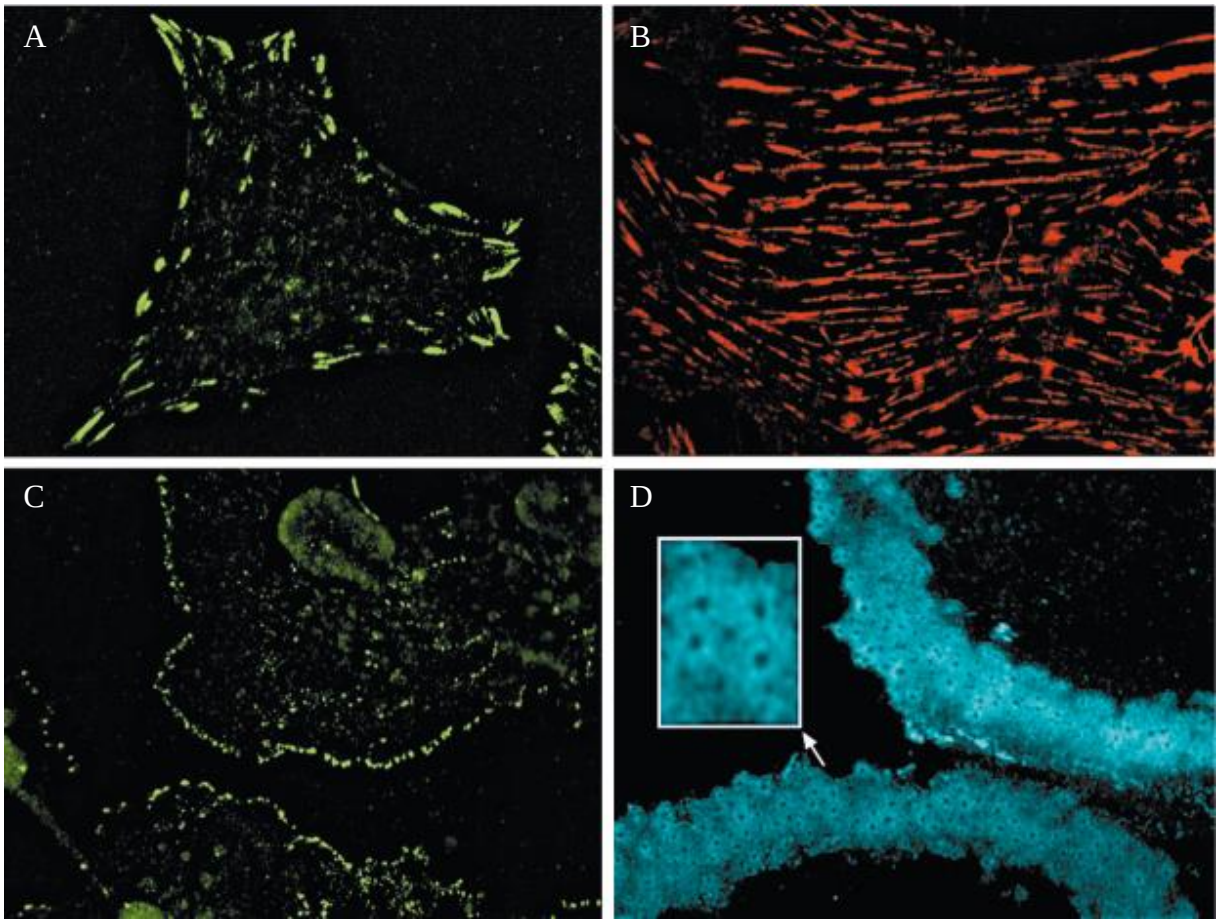

Figure 4: Various types of integrin-mediated adhesions. A – Classic focal adhesions in human foreskin fibroblasts labelled for phosphotyrosine. B – Fibrillar adhesions of human foreskin fibroblasts labelled for tensin. C – Focal complexes (dot-like structures) in human fibroblasts (SV80 line) treated with the Rho-kinase inhibitor Y-27632 and

labelled for phosphotyrosine. D – Podosomes in primary rat osteoclasts labelled for paxillin. Adopted from Geiger *et al.*, 2001 (97).

1.3.3.2 Selected proteins associated with focal adhesions

The whole integrin adhesome (a network of proteins associated with the integrin adhesion) consists of more than 230 proteins that mediate the link between the ECM and the cell cytoskeleton (99). In the following text, the focus will be on the crucial FA proteins that are involved in experimental work of this thesis: a) structural proteins - **talin** and **vinculin** b) signaling proteins - **FAK**, **Rho** proteins and extracellular signal-regulated kinases 1 and 2 (**ERK1/2**).

1.3.3.2.1 Talin

Talin is a large intracellular protein located mainly in FAs where is crucial for linking the integrin receptors to the actin fibres. Since the multidomain talin molecule contains binding sites for integrin, vinculin and actin (100, 101), it is believed that talin could serve as a molecular ruler that define FA architecture via stretch-induced recruitment of other proteins (93). Talin is also responsible for transmission of force from outside into the cell. Talin changes its conformation in response to force and this affects its interaction with particular ligands (100).

1.3.3.2.2 Vinculin

The adaptor protein vinculin is a crucial regulator of FA formation; it couples (together with talin) integrins to the actin cytoskeleton. It was shown that vinculin-null mouse embryo fibroblasts arranged smaller and less abundant FAs compared to the wild-type cells (102). Moreover, the vinculin-deficient cells or cells transfected with only part of vinculin (head or tail) exhibited reduced cell spreading and lamellipodium formation (103). These studies suggest that intact vinculin is essential for formation of classic FAs, lamellipodium development and proper cell spreading at all. Humphries *et al.* proposed a model of vinculin action (94). At the front of cell protrusion, vinculin is recruited to focal complexes by low-afinity binding to talin. Subsequently, the association of vinculin with actin or phosphatidylinositol (4,5)-bisphosphate causes vinculin activation. This vinculin activation includes integrin transition from the low-afinity state to the high-afinity state by binding to talin and results in stabilization of

activated integrins followed by growth of FAs. If vinculin activation does not occur, adhesion complexes disassembled promptly.

It was shown that vinculin activation is regulated by a spatial arrangement of particular protein interactions within FA at nanoscale (104).

1.3.3.2.3 Focal adhesion kinase

FAK is a non-receptor protein tyrosine kinase that plays a role in integrin signaling and cell spreading, migration, and apoptosis. FAK is activated by the autophosphorylation of the tyrosine-397 (pFAK-Y397) and also of other sites in the protein in response to integrin clustering and growth factor stimulation. This phosphorylation leads to the recruitment of many proteins containing SH2- and SH3-domains and subsequent signal transduction to downstream pathways within the cell resulting in changes in focal adhesion dynamics (105, 106). FAK acts as an adaptor protein for other proteins involved in FA formation, serves as an integrator of various signals and a regulator of assembling/disassembling of FAs and cell motility. FAK can affect also Rho GTPases involved in actin stress fibers formation via interaction with Rho activators or inhibitors. Moreover, the FAK signaling can modulate the formation of cell-cell contacts mediated by cadherins (107).

1.3.3.2.4 Rho proteins

Proteins of Rho family belong to Ras superfamily of GTPases. They are able to switch from the active GTP-bound state to the inactive GDP-bound state and hereby change a signal transduction chain on and off. They participate in the regulation of cell shape and polarity, migration and cell cycle cytokinesis through a regulation of cytoskeletal organization. The Rho family can be categorized into the three main subtypes including Cdc 42 (affects filopodia), Rac (affects lamellipodia) and Rho (affects stress fibres) subclasses (108, 109).

1.3.3.2.5 Extracellular signal-regulated kinases 1 and 2

The most of signals transmitted through FAs are transduced downstream by ERK1 and ERK2. They are also known as mitogen-activated protein kinase 3 and mitogen-activated protein kinase 1, respectively. Serin/threonin kinases ERK1 and ERK2 reveal 85% of sequence identity and are involved in the Ras-Raf-MEK-ERK signal transduction cascade. ERK1/2 proteins are activated by the phosphorylation on

two sites (threonine-202/tyrosine-204 or threonine-185/tyrosine-187, respectively) after the binding of growth factors or insulin on the membrane receptors and subsequent signal transduction upstream from the ERK proteins. Afterwards, the active ERK1/2 kinases phosphorylate many cytoplasmic and nuclear proteins including transcription factors. Thus, ERK1/2 proteins participate in the regulation of various processes, such as cell adhesion, migration, proliferation, metabolism and differentiation through the transmission of the extracellular signal to the nucleus (110, 111).

1.3.4 Glycocalyx

It should not be forgotten that, besides proteins, also sugars are presented on the cell surface. Sugars from membrane-bound glycoproteins, proteoglycans and glycolipids with integrated soluble molecules form glycocalyx, a layer covering cell membrane (112). The composition of glycocalyx is cell type specific. For many cells in tissue culture, the thickness of glycocalyx is 30 – 60 nm (113). Interestingly, the decrease in glycocalyx thickness was associated with dramatic increase in cell adhesion efficiency (114). Authors suggest that the glycocalyx reduction could be a convenient process for a cell how to rapidly increase the activity of many tens of membrane receptors. Therefore, the effect of glycocalyx on cell adhesion should be also taking in consideration. However, to simplify the very complex issue of cell adhesion, the glycocalyx is not investigated in the experimental section of this thesis.

1.4 Extracellular matrix

The ECM is a dynamic cell-free environment which undergoes a controlled remodeling. The function of ECM is to serve as an adhesive substrate for cells, to provide structure for tissue and organs development, to store growth factors and present them to cell receptors and also to transduce mechanical signals. The support from ECM is necessary for cell adhesion, migration, proliferation, communication, differentiation, morphogenesis, survival and for maintenance of tissue homeostasis and development (115). The information flow between ECM and cells is bidirectional. Cells are strongly affected by microenvironment of ECM and reversely, the cells remodel the adjacent ECM.

1.4.1 Composition of extracellular matrix

Two groups of macromolecules are present in ECM – proteoglycans and fibrous proteins (116). The proteoglycans are composed of sulfated glycosaminoglycan chains covalently connected to the core protein. One exception of this definition is hyaluronan, which is naturally not sulfated and not linked to a protein core. Proteoglycans are extremely hydrophilic and form hydrogel that enable the ECM to withstand strong compressive forces (117). The principal fibrous ECM proteins are collagens, elastins, fibronectins and laminins (116).

The main structural protein of ECM is collagen that is the most abundant protein in mammals constituting up to 30 % of total protein mass. The collagen molecules contain three α chains that form the triple helix. These trimeric molecules are secreted from the cells and then assembled into the supramolecular elongated fibrils or reticular networks and sheets which are incorporated into the ECM. The composition and organization of collagen fibrils and networks differ within the various tissues and create the characteristic patterns. Collagens exhibit high tensile strengths and therefore determine the strength and elasticity of tissues (118).

The adhesion-related proteins that are contained also in ECM and are studied in this thesis are FN and VN.

FN is a dimeric glycoprotein that is involved in cell adhesion, migration, growth, differentiation, wound healing and embryonic development. In humans, up to 20 variants of FN arise from alternative splicing of one pre-mRNA. Two main types of FN could be distinguished – soluble plasma FN and less-soluble cellular type which forms more heterogeneous group containing FNs with various properties. The cellular FN can assemble into a fibrillary network deposited in ECM. This highly regulated integrin-dependent process involves conformational changes of FN resulting in the exposition of fibronectin-binding sites which facilitates inter- and intramolecular interactions of FN. FN binds to integrins and also to syndecans, CD44, collagen, fibrin and other molecules presented in the ECM or the cell membrane (97, 119, 120).

VN is a small glycoprotein that is present in the blood serum and the ECM. This glycoprotein plays a role in cell adhesion, hemostasis and immune response. VN can bind integrins (promotion of cell adhesion, spreading and migration), collagens (anchoring to the ECM), heparin (involvement in blood clot formation), complement

proteins (inhibition of complement resulting in membrane attack repression), plasminogen and plasminogen activator inhibitor (involvement in fibrinolysis) (121).

1.4.2 Adhesion sequences in ECM proteins

The ECM proteins contain specific amino acid sequences that are recognized and bound by integrins located in cell membrane. The most widely known sequence is RGD (arginin-glycin-aspartic acid) mainly found in FN (122). The other adhesion sequences include e.g. GFOGER (glycine-phenylalanine-hydroxyprolin-glycine-glutamic acid-arginine) in collagen (123), YIGSR (tyrosine-isoleucine-glycine-serine-arginine) in laminin (124) or LDV (leucine-aspartic acid-valine) and REDV (arginine-glutamic acid-aspartic acid-valine) in FN (119).

KRSR (lysine-arginine-serine-arginine) is an example of non-integrin mediated adhesion sequence selectively recognized by transmembrane proteoglycans (e.g. heparan sulfate) of osteoblasts (125).

Not only adhesion sequence itself but also the spacing of these sequences and ligands affects the assembly of FAs and thus the cell spreading and cell fate. It was shown that the RGD spacing around 70 nm and more resulted in the poor formation of FAs, actin stress fibers, cell adhesion and spreading (126). Moreover, the effect of RGD nanospacing on differentiation of stem cells was reported. The large RGD nanospacing (approximately 90 nm) promoted the osteogenesis; whereas the small RGD nanospacing (approximately 40 nm) enhanced adipogenesis (127).

1.5 Fetal bovine serum

Cells are *in vitro* cultivated in the culture medium standardly supplemented by serum, most frequently by the fetal bovine serum (FBS). FBS is the blood fraction that remains after blood coagulation. It contains various proteins and factors important for cell adhesion, proliferation and survival such as growth factors, adhesion-mediating factors (e.g. FN, VN, laminin), vitamins, hormones, cofactors, transport factors (e.g. albumin, transferrin) and nutrients (nucleosides, amino and fatty acids, lipids) (128). Although it is obvious that *in vitro* cultivation cannot be the same as natural conditions for cell existence, the use of FBS should at least partially mimic the chemical environment of *in vivo* conditions. First, the proteins of FBS adsorb to the substrate fast and only afterwards, the cells adhere to the adsorbed protein layer (129). Thus, the cell adhesion is *in vitro* strongly influenced by the proteins of FBS. The reason for usage of

fetal serum instead of serum from adults or newborns is that fetal serum contains more growth factors and lower level of complement.

In bio-medical applications, the usage of FBS is problematic due to its high batch-to-batch variability, the possible transmission of fungal, bacterial, viral or prion infection (therefore FBS is tested for the presence of many microbes), and the possibility of anti-FBS antibody production (130). Also the ethical aspect of FBS extraction could not be neglected. Therefore, as alternatives for FBS usage, serum-free media for defined and controlled *in vitro* culture conditions have been developed (131). However, these serum-free media are cell specific and must be optimized, resulting in the higher costs. Thus, despite certain drawbacks, FBS usage is quite universal, extremely effective and the most widespread option for *in vitro* cell cultivation.

1.5.1 Cell adhesion onto fetal bovine serum proteins

The most abundant protein in FBS is BSA (more than 50 % of FBS protein content) which has an important impact on protein competition for attachment to any surface. BSA is a small (66 kDa) globular protein that negatively affects cell adhesion, predominantly onto hydrophobic surfaces (55).

The other FBS proteins mediating the cell adhesion and being also a part of the ECM are FN and VN. It was reported that adsorption of VN on substrate in cell cultures containing FBS was increased compared to FN (132). It has been also shown, that FN failed to coat the substrate in the presence of other serum proteins in contrast to VN that was able to coat the surface under the same conditions (133). It could be suggested that VN is the leading cell adhesion-promoting protein of FBS. Moreover, different appearance and distribution of FAs were observed in cells cultivated on VN and FN. FAs in the cells cultivated on VN had large and peripherally distributed FAs. In contrast, FN induced relatively smaller FAs distributed over the whole cell (Fig. 5). Moreover, VN caused smaller cell spreading compared to FN (78). Both FN and VN contain the RGD sequence, which is recognized and bound by specific integrins (122).

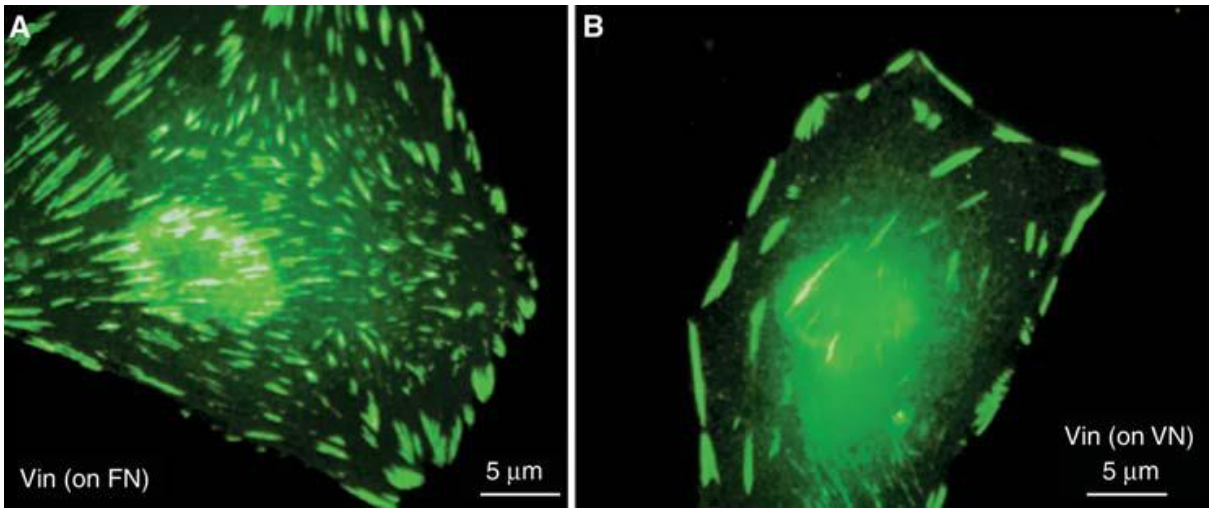

Figure 5: Effect of fibronectin and vitronectin on cell spreading and FA formation. Vinculin-labeled adhesions in fibroblasts adhered to fibronectin (A) or to vitronectin (B). Adopted from Geiger and Yamada, 2011 (78).

Generally, it is believed that FBS proteins compete for adsorption to a surface and that cell adhesion is influenced by the balance between adhesion-promoting (e.g. FN) and adhesion-inhibiting (e.g. BSA) proteins. Moreover, FN can compensate for the negative effect of BSA.

Finally, all factors such as the type of proteins present in the cell cultivation environment, their quantity and conformation significantly affect cell adhesion and subsequent cell behavior.

1.6 Cryopreservation of cells

The cryopreservation of cells is essential method for everyone who works with cell cultures. Cryopreservation assures the protection of cells before degradation, damaging, aging and contamination by stopping of all enzymatic and chemical activity in frozen sample, standardly in liquid nitrogen (-196°C). The question is how to ensure that cells survive both, the freezing to -196 °C and the subsequent return to the cultivation conditions (134). The biggest problem during freezing is the formation of intracellular ice crystals which mechanically damage the cells.

To minimize the lethal effect of freezing and thawing of cells, various cryoprotectants are added to the freezing medium. Cryoprotectants protect the cells before ice crystals-associated damage by increasing of solute concentration. The disadvantage of most of cryoprotectants is their cytotoxicity (135). Besides the

treatment by cryoprotectants, the slow gradual cooling also helps to prevent the cell damage during freezing procedure by allowing the sufficient water to leave the cell. The ideal cooling rate should be optimize for each cell or tissue type, but the typical cooling rate for mammalian cultures is around 1°C/minute (134, 136). After thawing, the cells should be cultivated in optimal conditions for a certain time before using them for experiments or administration into animals or humans as has been demonstrated by Francois *et al.* (137). The authors showed that freshly thawed human mesenchymal stromal cells temporarily lost their ability to suppress T cell activation. However, this capability was fully restored after 24 h of cultivation of thawed cells on culture polystyrene at 37°C with 5% CO_2 which suggests the need of some time to renewal of cell functions after thawing (137).

1.6.1 Cryoprotectants

Cryoprotectants could be divided into two groups: intracellular agents and extracellular agents. The intracellular agents such as dimethyl sulfoxide (DMSO), glycerol or ethylene glycol penetrate into cells where prevent the ice crystals formation. The extracellular agents such as sucrose, trehalose or raffinose persist outside the cell and balance the osmotic pressure that occurs during freezing. Generally, it is believed that the intracellular agents are more effective. For example, Janz *et al.* showed that DMSO and glycerol (the intracellular cryopreservation agents) provided more protective effects for mesenchymal stem cell viability than sucrose or trehalose (the extracellular cryopreservation agents). Whereas the expression of stem cells surface markers and the potential to differentiation remained unaffected (138).

The most widely used cryoprotectant is DMSO; however, high concentration of DMSO causes cellular toxicity through plasma membrane pore formation (139) and/or stimulation of apoptosis through inhibition of mitochondrial respiration and increasing of intracellular calcium (140). The particular cytotoxic DMSO concentration depends on the cell type, the time of exposure and the temperature during exposure (136, 141). In addition, also FBS is often part of freezing medium. However, the usage of FBS is often undesirable primarily for clinical applications because of the possible transmission of prion and other zoonotic infections. It is possible to obtain FBS from countries free of bovine spongiform encephalopathy; however these products are more expensive. Moreover, FBS is a poorly understood substance with inherent variation between sources and batches. On that account, the alternative cryoprotectants are tested such as

sericin (silk protein) (142), dextran 40 (143), polyvinylpyrrolidone (144) or poly-L-lysine (145).

1.6.1.1 Sericin as a cryoprotectant

Sericin is an amorphous sticky glycoprotein derived from the silkworm (Bombyx mori) cocoon. It is the second major protein component (besides fibroin) of silk and is extracted from the cocoon by a degumming process (a thermo-chemical process) – the most efficiently by using of a sodium carbonate salt-boiling system (146). Sericin is rich in the amino acid serine and is water soluble (147).

Sericin has a number of attractive properties that are the subject of current research involving e.g. the promotion of mouse fibroblasts viability and collagen production at certain sericin concentrations (148), the acceleration of mammalian cells proliferation and production of monoclonal antibodies by hybridoma cells (149) or the suppression of skin tumorigenesis (150) and colon carcinogenesis (151) in murine models. In addition, a great advantage of sericin is that silk has been approved as a biomaterial by the US Food and Drug Administration (152).

Sericin can be used as a cryoprotectant instead of FBS during freezing of various cell types such as human adipose tissue-derived stem cells (153), myeloma cell lines, ovarian cells, fibroblasts, keratinocytes and insect cell lines (142), rat insulinoma cell lines, and mouse hybridoma cell lines (154). Wu *et al.* revealed that purified sericin antifreeze peptide (named SM-AFP) with the sequence of TTSPTNVSTT is responsible for prevention of ice crystal growth owing to hydrogen bond formation, hydrophobic interactions and non-bond interactions between the peptide and ice (155). Thus, this peptide could be used as a cryoprotectant instead of whole sericin.

Based on the literature, it seems that sericin can be an adequate replacement for FBS during a freezing of cells; however, the use of sericin as a cryoprotectant should be always evaluated for a particular cell type and experimental set-up.

2 AIMS OF THE THESIS

I. To characterize the behavior of osteoblasts on differently treated graphene and nanocrystalline diamond, with regard to cell adhesion and proliferation in the presence and the absence of FBS proteins.

II. To characterize an early phase of cell adhesion with respect to the presence or absence of FBS. To compare early cell adhesion of immortalized cell line and primary cells.

III. To evaluate sericin as a substitute for FBS in a freezing medium for immortalized cell line and primary cells.

3 MATERIALS AND METHODS

All used materials and methods are described in detail in publications A-E. As regards these publications, here is presented a list of used methods that were performed by me and that belong to the biological part of this thesis. Materials and methods that are not described in publications A-E are specified below in a full form.

- Tested materials
    - Nanocrystalline diamond (NCD) on silicon substrate
        - NCD treated with oxygen plasma (NCD-O)
        - NCD treated with hydrogen plasma (NCD-H)
    - Graphene (G) on silicon substrate
        - Single-layer G treated with H_2/Ar (1-LG)
        - Single-layer G treated in an oxidizing atmosphere (1-LG-O)
- Culture of cells
    - Human osteoblast-like cell line (SAOS-2) (in Publications A-E)
    - Human dermal fibroblasts
    - Human mesenchymal stem (stromal) cells (in Publication E)
- (Immuno)fluorescence staining of cells, stained structures:
    - Nuclei (in Publications A-E)
    - Actin stress fibers (in Publications A-D)
    - Vinculin (in Publications A-D)
    - CD44 (in Publication D)
    - Talin (in Publication D)
    - pFAK-Y397 (in Publication D)
    - Rho (Y486) (in Publication D)
    - pERK1/2 (in Publication D)
- Cell imaging by fluorescence microscopy (in Publications A-E)
- Advanced image analyses
    - Cell number determination (in Publications A-E)
    - Cell area determination (in Publications A-D)
    - Analysis of focal adhesions (in Publication B)
    - Measurement of fluorescence intensity (in Publication D)

    - ImageJ (Rasband, W.S., ImageJ, U.S. National Institutes of Health, Bethesda, Maryland, USA, http://imagej.nih.gov/ij/, 1997-2016) and Cell Profiler (Broad Institute, USA) softwares were used.
- Cell adhesion strength determination (in Publication D)
- CFU-F assay (colony-forming unit-fibroblast) (in Publication E)
- Protein pre-adsorption on glass surfaces (in Publication D)
- Cryopreservation of cells (in Publication E)
- Statistical analyses
    - One-way ANOVA (in Publication A)
    - Nonparametric Mann-Whitney U test (in Publications B and C)
    - Wilcoxon signed-rank test (in Publication E)
    - STATISTICA Software (StatSoft, Czech Republic) was used

3.1 Inhibition of integrins

NCD samples were sterilized by 70% ethanol for 10 min and afterwards washed by sterile demineralized water three times. SAOS-2 cells (50 000/cm^2) were harvested and centrifuged (300g, 7 min, 25°C). Cells were resuspended in medium without FBS and with antibody anti αVβ5 (final concentration 20 ug/ml; mouse monoclonal antibody anti human integrin αVβ5, RD Systems, USA) or antibody anti α5β1 (final concentration 20 ug/ml; mouse monoclonal antibody anti human integrin α5β1 [P1D6], Abcam, United Kingdom) or without any inhibition antibody as a control. Cells were incubated in water bath (37°C) for 10 min and shaken in hand every minute. Afterwards, FBS was added to cells (final concentration 15 %) and cells (400 µl) were seeded onto 24-well plate (TPP, Switzerland).

3.1.1 Fluorescence staining

After 2 h, cells were fixed by 4% paraformaldehyde at room temperature (RT) for 15 minutes and nuclei and actin filaments were fluorescently stained. Cells were permeabilized by Triton X-100 (0,1%) at RT for 20 min. Cell nuclei were stained with 4',6-diamidino-2-phenylindole (DAPI, 1:1000, Sigma-Aldrich, USA) and actin filaments with phalloidin conjugated with Alexa Fluor 488 (1:500, Life Technologies, USA). Fluorescence images of cells were obtained using Eclipse Ti-S microscope (Nikon, Japan) and DS-Qi1Mc Digital Camera (Nikon, Japan).

3.1.2 Statistical analysis

Cell number and cell area were calculated from ten images. Due to rejection of normal distribution of assessed data, the non-parametric Kruskal-Wallis ANOVA with subsequent post-hoc test based on pair-wise comparisons with the Bonferroni correction was used for determination of significant differences between the datasets. P values of less than 0.05 were considered to be statistically significant. STATISTICA Software (StatSoft, Czech Republic) was used for these statistical analyses.

3.2 qRT-PCR (quantitative polymerase chain reaction with reverse transcription)

NCD samples were sterilized by 70% ethanol for 10 min and afterwards washed by sterile demineralized water three times. SAOS-2 cells (30 000/cm^2) were harvested and centrifuged (300g, 7 min, 25°C). Cells were resuspended in medium with 15% FBS or without FBS and seeded onto NCD samples in duplicates. After 2 h, total RNA was isolated from cells using RNeasy Plus Micro Kit (Qiagen, Germany) according to the manufacturer´s protocol.

Isolated RNA was analyzed on NanoDrop spectrophotometer ND-1000. Isolated RNA (50 ng) was used for reverse transcription (RT) by means of SuperScript III Reverse Transcriptase (Thermo Fisher Scientific, USA) according to the manufacturer´s protocol. Each qPCR reaction was performed in tetraplicates on a LightCycler 480 (Roche, Germany) using Universal Probe Library System Technology (Roche, Germany). The cDNA was diluted 5x prior to use in qPCR reaction as a template. Controls with no template were used in each qPCR reaction. Primers used in qPCR are listed in Table 1.

qPCR data were analyzed by means of Double Delta Ct method (relative quantification) (156). All qPCR data (Ct values – cycle threshold) were normalized to geometrical mean of three housekeeping genes. Afterwards, data from osteoblasts cultivated on tissue culture polystyrene (TCPS) with FBS were considered to be a calibrator (standard) and all other data were normalized to this calibrator. Three independent experiments were done and the specific expression level of tested gene was considered to be relevant if the same result was observed in at least two experiments.

Housekeeping genes		
Human GAPDH	forward primer	5'- AGCCACATCGCTCAGACAC - 3'
	reverse primer	5'- GCCCAATACGACCAAATCC - 3'
Human HPRT1	forward primer	5'- TGACCTTGATTTATTTTGCATACC - 3'
	reverse primer	5'- CGAGCAAGACGTTCAGTCCT - 3'
Human HMBS	forward primer	5'- CTGAAAGGGCCTTCCTGAG - 3'
	reverse primer	5'- CAGACTCCTCCAGTCAGGTACA - 3'
Tested genes		
Human integrin α1	forward primer	5'- AATTGGCTCTAGTCACCATTGTT - 3'
	reverse primer	5'- CAAATGAAGCTGCTGACTGGT - 3'
Human integrin α2	forward primer	5'- TCGTGCACAGTTTTGAAGATG - 3'
	reverse primer	5'- TGGAACACTTCCTGTTGTTACC - 3'
Human integrin α3	forward primer	5'- GAGGACATGTGGCTTGGAGT - 3'
	reverse primer	5'- GTAGCGGTGGGCACAGAC - 3'
Human integrin α5	forward primer	5'- CCCATTGAATTTGACAGCAA - 3'
	reverse primer	5'- TGCAAGGACTTGTACTCCACA - 3'
Human integrin αV	forward primer	5'-CATGTCCTCCTTATACAATTTTACTGG - 3'
	reverse primer	5'- GCAGCTACAGAAAATCCGAAA - 3'
Human integrin β1	forward primer	5'- CGATGCCATCATGCAAGT - 3'
	reverse primer	5'- ACACCAGCAGCCGTGTAAC - 3'
Human integrin β3	forward primer	5'- CGCTAAATTTGAGGAAGAACG - 3'
	reverse primer	5'- GAAGGTAGACGTGGCCTCTTT - 3'
Human integrin β5	forward primer	5'- GGAGTTTGCAAAGTTTCAGAGC - 3'
	reverse primer	5'- TGTGCGTGGAGATAGGCTTT - 3'

Table 1: PCR primers used for qPCR. GAPDH - glyceraldehyde-3-phosphate dehydrogenase, HPRT 1 - hypoxanthine phosphoribosyltransferase 1, HMBS - hydroxymethylbilane synthase

3.3 Transcriptomic profiling

SAOS-2 cells (15 000 cells/cm^2) were plated onto TCPS with and without FBS in duplicates. After 2 h, total RNA was isolated from cells using RNeasy Plus Micro Kit (Qiagen, Germany) according to the manufacturer´s protocol. The quality of the total RNA was evaluated using an Agilent 2100 Bioanalyzer system (Agilent, USA). Microarray experiments were performed using the Affymetrix Human Gene 2.1 ST Array Strips processed by Affymetrix GeneAtlas system (Affymetrix, USA) according to the manufacturer´s protocol. Acquired data were analyzed through the use of Partek Genomics Suite 6.6 (Partek, St. Louis, Missouri). The data were normalized by Robust Multichip Average algorithm, which uses background adjustment, quantile normalization and summarization. Pathway and network analysis including assessment of overrepresentation of differentially expressed probes in canonical, metabolic and signalling pathways and ontological classes, common regulator effects and in silico network construction was performed using the Ingenuity Pathways Analysis software (IPA, www.qiagen.com/ingenuity). Except the culture of cells and isolation of RNA, all steps were performed by colleagues from Institute of Biology and Medical Genetics of the First Faculty of Medicine.

3.4 Transfection of cells

SAOS-2 cells were transfected by DNA plasmid pGZ21 containing full-length chicken vinculin cDNA linked with green fluorescent protein (GFP) coding sequence under cytomegalovirus promoter control (157). The transfection was performed using Lipofectamine 2000 (Thermo Fisher Scientific, USA) according to the manufacturer's instructions. Stable expression of vinculin-GFP was achieved using selective medium containing geneticin G418 (0.6 mg/ml; Thermo Fisher Scientific, USA). For achievement of cells with stable gene expression from monocolony, cells were seeded into 96-well plate at very low concentration (500 cells/plate) 90 days after application of selective medium.

3.5 Live-cell imaging

A dish with thin glass bottom (WillCo Wells B.V., Netherlands) was placed into a chamber in Okolab system for live-cell microscopy (Okolab, Italy) with controlled environment (37°C and 5% CO_2). Afterwards, SAOS-2 cells with stable expression of vinculin-GFP (20 000 cells/cm^2) were plated onto prepared dish and imaged for 48 h

using a Nikon TE2000E microscope (Nikon, Japan). Images were captured using CFI Apo TIRF 60X Oil objective (N.A. 1.49; Nikon, Japan) and 488 nm excitation laser (Nikon, Japan). The emission of fluorophore was detected using 515/30 nm band-pass filters. Moreover, cells were imaged also using differential interference contrast (Nomarski interference contrast).

3.6 Adhesion experiments with primary human fibroblasts and human mesenchymal stem cells

3.6.1 Primary human fibroblasts

Normal human dermal fibroblasts (NHDF) were isolated from facial skin removed during cosmetic plastic surgery from donors after providing informed, written consent in collaboration with hospital Lochotín, Czech Republic. NHDF were obtained from the dermis by the digestion method (158). Fibroblasts were cultivated in Dulbecco's modified Eagle's medium–low glucose (DMEM) medium (Thermo Fisher Scientific, USA) supplemented with 10% heat inactivated FBS (PAA, Austria), penicillin (20 U/ml; Sigma-Aldrich, USA), streptomycin (20 mg/ml; Sigma-Aldrich, USA), D-glucose (2 g/l; Thermo Fisher Scientific, USA) and L-glutamine (2 mM; Thermo Fisher Scientific, USA) at 37 °C and in a 5% CO2 atmosphere. NHDF in the 3rd – 4th passage were used for experiments.

3.6.2 Human mesenchymal stem cells

Human mesenchymal stem cells (hMSCs) were obtained from healthy donors after providing informed, written consent. Bone marrow blood was aspirated from the posterior iliac crest and the mononuclear fraction was isolated by gradient centrifugation. The adherent cells were cultivated in a-MEM medium (Thermo Fisher Scientific, USA) with 10% heat inactivated FBS (PAA, Austria), penicillin (20U/mL; Sigma-Aldrich) and streptomycin (20 mg/mL; Sigma-Aldrich). Experiments were performed with hMSCs from two donors in passage number one.

3.6.3 Cell seeding

Cells were collected at 50 – 90% confluence using trypsin (Thermo Fisher Scientific, USA), washed in FBS-free medium and resuspended in medium with 10%

FBS or FBS-free medium. Cells were seeded onto tissue culture polystyrene (TPP, Switzerland) at a density of 15 000 cells/cm^2 and cultivated for 2 h.

3.6.4 Immunofluorescence staining

After 2 h, cells were fixed and imunofluorescently stained as described in Publication D.

3.6.5 Statistical analysis

As regard cell number and cell area, the nonparametric Mann-Whitney U test was used to determine the significant differences between the datasets, and p-values of less than 0.01 were considered as statistically significant. STATISTICA Software (StatSoft, Czech Republic) was used for these statistical analyses.

4 RESULTS

4.1 List of original publications used for PhD thesis

A) **Martina Verdanova**, Antonin Broz, Martin Kalbac, Marie Kalbacova (2012): Influence of oxygen and hydrogen treated graphene on cell adhesion in the presence or absence of fetal bovine serum. Phys. Status Solidi B 249, 12, 2503–2506. IF_{2012} = 1.489

B) Marie Hubalek Kalbacova, **Martina Verdanova**, Antonin Broz, Aliaksei Vetushka, Antonin Fejfar, Martin Kalbac (2014): Modulated surface of single-layer graphene controls cell behavior. Carbon 72, 207-214. IF_{2014} = 6.196

C) **Martina Verdanova**, Bohuslav Rezek, Antonin Broz, Egor Ukraintsev, Oleg Babchenko, Anna Artemenko, Tibor Izak, Alexander Kromka, Martin Kalbac, Marie Hubalek Kalbacova (2016): Nanocarbon Allotropes - Graphene and Nanocrystalline Diamond - Promote Cell Proliferation. Small 12, 18, 2499–2509. IF_{2014} = 8.368

D) **Martina Verdanova,** Pavla Sauerova, Ute Hempel, Marie Hubalek Kalbacova (2016): The effect of serum proteins on initial osteoblast adhesion. Biochemistry and Cell Biology – submitted

E) **Martina Verdanova**, Robert Pytlik, Marie Hubalek Kalbacova (2014): Evaluation of Sericin as a Fetal Bovine Serum-Replacing Cryoprotectant During Freezing of Human Mesenchymal Stromal Cells and Human Osteoblast-Like Cells. Biopreservation and Biobanking 12, 2, 99-105. IF_{2014} = 1.340

Above mentioned publications are included in a full form in this PhD thesis. For a complete list of articles with my contribution see the Complete list of my publications.

4.2 Publications A-C

The Publications A-C are focused on behavior of human osteoblasts (SAOS-2 cells, cell line derived from the primary osteosarcoma) cultivated on large-scale graphene (G, Publication A-C) or nanocrystalline diamond (NCD, Publication C) for a short time (2 h) and a longer time (48 h). Bone implant coating or cellular sensors are the possible applications of these carbon nanomaterials in terms of the research in this thesis. For this reason, basic information on cell interactions with these materials is essential and thus far only little explored.

In this thesis, cell adhesion on G and NCD is characterized under two conditions:

1) **Standard conditions** - in the presence of FBS that forms protein layer on materials fast and cells adhere rather on this protein layer than on plain material itself
2) **Non-standard conditions** - in the absence of FBS, the cells adhere directly on the plain material

This research has an interdisciplinary character and is composed of two parts – biological and material. The biological part of this complex research was performed by me and will be presented in this thesis predominantly. The material part of this research was performed by colleagues from J. Heyrovsky Institute of Physical Chemistry of the Czech Academy of Sciences and Institute of Physics of the Czech Academy of Sciences. For a full understanding of the research in this thesis, the material part will be also presented; however less than biological part.

4.2.1 Publication A: Influence of oxygen and hydrogen treated graphene on cell adhesion in the presence or absence of fetal bovine serum

Martina Verdanova, Antonin Broz, Martin Kalbac, Marie Kalbacova (2012): Influence of oxygen and hydrogen treated graphene on cell adhesion in the presence or absence of fetal bovine serum. Phys. Status Solidi B 249, 12, 2503–2506. IF_{2012} = 1.489

A groundbreaking discovery and description of electrical properties of a new material - graphene was published in Science in 2004 (9). In 2010, Andre Geim and Konstantin Novoselov were awarded by the Nobel Prize in Physics for "groundbreaking experiments regarding the two-dimensional material graphene". Based on graphene exciting properties (at once very thin and strong material), graphene has promised many fascinating applications in electronics. Luckily, my tutor had access to this great material and had started the experiments with regard to cell cultivation on graphene for possible applications in biology and medicine. These fundamental experiments demonstrated that CVD-grown graphene (without additional surface treatment) was suitable substrate for cultivation of human osteoblasts and mesenchymal stem cells (21). Based on these promising results, my research has started with a study of behavior of human osteoblasts on differently treated graphene (Publication A).

A focus in Publication A was on osteoblast adhesion at 2 h after cell seeding on hydrogen treated (hydrophobic) or oxygen treated (hydrophilic) graphene. This was the first time when graphene was modified by this way. Osteoblast adhesion was characterized in the presence of FBS (standard conditions) and in the absence of FBS (non-standard conditions).

The used graphenes were characterized by contact angle measurement: graphene that was treated with hydrogen demonstrated hydrophobic properties (CA 90°) whereas graphene treated with oxygen exhibited hydrophilic properties (CA 58°). Interestingly, the control tissue culture treated polystyrene (TCPS) revealed the same CA (58°) as graphene treated with oxygen.

The osteoblast adhesion was investigated by visualization of a) cell nuclei in order to cell number determination, b) actin filaments in order to cell area assessment and c) vinculin for characterization of cell focal adhesions using fluorescence microscopy and advanced image analysis.

It was shown that larger differences were observed between osteoblast adhesion in the presence and absence of FBS than between hydrogen and oxygen treated graphenes. Osteoblasts had star-like shape and larger cell area on all substrates (both types of graphene and TCPS used as control) in the absence of FBS compared to substrates where protein layer from FBS was formed (Fig. 1 and 2 in the enclosed Publication A). Moreover, higher amount of cells adhered on both graphenes in FBS absence compared to FBS presence after 2 h of cultivation (Fig. 2 in the enclosed Publication A).

As regards cell size, osteoblasts on graphene treated with hydrogen showed larger cell area than cells on graphene treated with oxygen. This was the only difference in osteoblast behavior on variously treated graphenes.

In this initial paper, the first promising findings about adhesion of osteoblasts on hydrogen or oxygen treated graphene after 2 h in the presence or absence of FBS were described. However, we were interested in cell reactions also after longer time period. Moreover, the used graphenes were characterized by contact angle measurement in this paper; however, an additional material characterization was not accomplished due to not yet developed techniques for determination of properties of this fine one atom thick layer carbon material. For these reasons, our research continued with a characterization of cell behavior after longer time period (48 h) and more detailed characterization of cell adhesion on researched materials after short time period (2 h). In addition, other important characterization of used graphenes was carried out. These results are presented in publication B.

4.2.2 Publication B: Modulated surface of single-layer graphene controls cell behavior

Marie Hubalek Kalbacova, **Martina Verdanova**, Antonin Broz, Aliaksei Vetushka, Antonin Fejfar, Martin Kalbac (2014): Modulated surface of single-layer graphene controls cell behavior. Carbon 72, 207-214. IF_{2014} = 6.196

This paper builds on previous encouraging studies (Publication A) about osteoblast adhesion on differently treated graphenes after 2 h of cultivation and extends the previous observations. In addition, we wanted to know how osteoblasts will react on their cultivation on the same graphene samples after longer time (48 h). Similarly to the Publication A, we researched hydrogen treated (1-LG, hydrophobic) and oxygen treated (1-LG-O, hydrophilic) graphene.

Here, we were focused on deeper characterization of used graphenes. The roughness of both graphene samples (1-LG and 1-LG-O) on underlying substrate (pristine SiO_2/Si) was characterized using atomic force microscopy (AFM). Visible nanowrinkles on both graphenes were observed (Fig. 1 in the enclosed Publication B). A roughness of 1-LG (2.03 nm) was slightly higher than of 1-LG-O (1.05 nm). Furthermore, properties of the graphenes samples were described using Raman spectrometer. The Raman measurement indicated a slightly increased amount of defects on 1-LG-O than in 1-LG that could result in different charge characteristics of both graphenes (Fig. 2 in the enclosed Publication B). These all material measurements were performed by colleagues from J. Heyrovsky Institute of Physical Chemistry of the Czech Academy of Sciences and Institute of Physics of the Czech Academy of Sciences.

Our biological group was focused on osteoblast behavior on this hydrogen treated (1-LG, hydrophobic) and oxygen treated (1-LG-O, hydrophilic) graphene after 2 h and 48 h of cultivation. We used the same molecular biology methods as in publication A, i.e. fluorescence microscopy with advanced image analysis. The larger role of FBS than of graphene treatment on cell adhesion on graphenes after 2 h of cultivation was confirmed. However, after 48 h of cultivation, the differences between cell behavior on differently treated graphenes were observed, namely more and larger

cells were detected on 1-LG than on 1-LG-O. 1-LG promoted cell proliferation as well as cell spreading (Fig. 5 and 6 in the enclosed Publication B).

For 48 h of cell cultivation, the non-standard conditions mean that FBS was not present in medium during first 2 h. However, since FBS is essential for cell survival during longer cultivation, FBS was added to cells after first 2 h. Thus, additional 46 h of cell cultivation proceeded in the presence of FBS.

As regards role of FBS, it seems that FBS has a negative effect on cell adhesion because of more and larger cells adhered on both graphenes in FBS absence. Contrary, after 48 h of cell cultivation, cells that adhered in FBS absence are inhibited in cell proliferation and spreading despite the fact that the FSB was present in medium for additional 46 h of cell cultivation (Fig. 5 and 6 in the enclosed Publication B).

In this paper, cell adhesion was also analyzed for number of FAs, average area of a single FA and percentage of area covered by FAs in individual cells after 48 h of cell cultivation. Cells on 1-LG-O in FBS presence had a smaller number of larger FAs (forming clusters) compared to other substrates. However, despite various individual FA number and size, the same adhesion area of cells was comparable on most of the tested samples (Fig. 7 in the enclosed Publication B).

Thus, it was shown that 1-LG and 1-LG-O have diverse properties (wettability, roughness, and defects) that affect cell behavior, especially after longer cultivation (48 h). Various cell behavior is also affected by the proteins originated from FBS that probably adhere differently on variously modified graphenes.

Based on these attractive results, more experiments with 1-LG and 1-LG-O and human osteoblasts were performed to confirm the obtained results. Moreover, osteoblast behavior on another carbon nanomaterial – nanocrystalline diamond – was studied and compared to cell behavior on graphenes. These results are presented in publication C.

4.2.3 Publication C: Nanocarbon Allotropes - Graphene and Nanocrystalline Diamond - Promote Cell Proliferation

Martina Verdanova, Bohuslav Rezek, Antonin Broz, Egor Ukraintsev, Oleg Babchenko, Anna Artemenko, Tibor Izak, Alexander Kromka, Martin Kalbac, Marie Hubalek Kalbacova (2016): Nanocarbon Allotropes - Graphene and Nanocrystalline Diamond - Promote Cell Proliferation. Small 12, 18, 2499–2509. IF_{2014} = 8.368

In the previous two publications (A and B), we showed exciting differences in osteoblast behavior when they are cultivated on hydrogen-treated (hydrophobic) and oxygen-treated (hydrophilic) graphene. Moreover, a big role of initial absence of FBS on osteoblast adhesion and proliferation was demonstrated as well. Based on these attractive findings we were curious how osteoblasts will react to another carbon nanomaterial – nanocrystalline diamond, in fact the chemically same material as graphene and with similar application potential; however with different arrangements of carbon atoms.

This paper describes human osteoblast behavior on two different carbon allotropes – NCD and G. The same hydrogen treated graphene (hydrophobic 1-LG) and oxygen treated graphene (hydrophilic 1-LG-O) as in publication A and B were used. The studied NCDs were also divided into two types – hydrogen treated NCD (hydrophobic NCD-H) and oxygen treated NCD (hydrophilic NCD-O). The different treatment of G and NCD (by hydrogen or oxygen) results in various wettability (hydrophobicity or hydrophilicity) that can have a great impact on cell behavior.

Studied G and NCD were characterized in detail by scanning electron microscopy (SEM), AFM, Raman microspectroscopy, X-ray photoelectron spectroscopy and contact angle measurement that were performed by colleagues from J. Heyrovsky Institute of Physical Chemistry of the Czech Academy of Sciences and Institute of Physics of the Czech Academy of Sciences.

Based on AFM measurements, it was shown that 1-LG-O had low roughness (5 ± 2 nm), comparable to control TCPS. 1-LG revealed slightly higher degree of roughness (9 ± 3 nm) than 1-LG-O. Both NCD films had even higher roughness (20 ± 3 nm); however, the values were still within the nanoscale (Tab. 1 in the enclosed Publication C). Although the equally prepared 1-LG and 1-LG-O were used in Publication B and

Publication C, slightly diverse roughness (RMS) were acquired (2.03 nm and 9 ± 3 nm for 1-LG / 1.05 nm and 5 ± 2 nm). This dissimilarity could be caused by the fact that both measurements were performed by various persons from various institutes with subtle differences in used methods. Moreover, the AFM measurements here were carried out in more detail, because of more developed techniques during the time.

If we took together data from SEM (surface morphology) and AFM (surface roughness – RMS and skew/kurtosis values), we were able to depict the schematic cross-sectional representations of the surface morphologies on studied NCD and G (Fig. 1 in the enclosed Publication C). The principal conclusion of these challenging studies about surface topography of NCD and G was theory that 1-LG-O is almost flat substrate; 1-LG has nanowrinkled morphology and both NCDs are relatively rough (in nanoscale) surfaces.

Based on contact angle measurement, the most hydrophilic material was NCD-O (15°) followed by 1-LG-O (58°), which had the same CA as control TCPS. On the other hand, the most hydrophobic material was NCD-H (100°) followed by 1-LG (90°) (Tab. 1 in the enclosed Publication C).

Osteoblast behavior was investigated on these 4 nanomaterials (1-LG, 1-LG-O, NCD-O and NCD-H) and control TCPS in the presence or initial absence of FBS for 2 h and 48 h of cultivation. Repeatedly, immunofluorescence staining of nuclei and actin filaments followed by fluorescence microscopy with advanced image analysis were methods used in this publication.

Since many variables were examined, the effect of nanomaterial (NCD versus G) irrespective of their particular surface treatment and only in the presence of FBS during whole time was presented at first. It was shown that fewest cells adhered to G and these cells were the smallest ones. On the other hand, cells on G revealed superior proliferation in comparison to NCD (Fig. 5 in the enclosed Publication C). In more detailed point of view, it was demonstrated that behind the accelerated cell proliferation on G, more properties of 1-LG were present than of 1-LG-O. However, 1-LG-O still promoted cell proliferation more than both NCD. Similar degrees of cell adhesion and proliferation were observed on hydrophilic NCD-O and hydrophobic NCD-H (Fig. 6 in the enclosed Publication C).

When cells adhere on studied materials in the absence of FBS, comparable numbers of cells were detected on all the tested substrates that are in contrast to standard conditions with FBS presence in medium. Generally, around twice as many

cells adhered to all the substrates in the absence of FBS than in its presence, which suggests that FBS reduces cell adhesion. This observation is in agreement with results from publications A and B. It was shown again that the lack of FBS for the first 2 h of cultivation suppresses further cell proliferation (Fig. 7 in the enclosed Publication C). However, the highest cell proliferation on 1-LG was detected under non-standard conditions (FBS absence during first 2 h of cultivation) as well under standard conditions (FBS presence during whole time of cultivation). This is advantage in terms of the potential use of 1-LG as bioelectronics sensor and actuator where protein interlayers often affect sensor performance.

4.3 Detailed characterization of osteoblast adhesion on nanocrystalline diamond

The previous study of our group (60) showed that cells those adhered on nanocrystalline diamond (NCD) samples with hydrophilic/hydrophobic stripes (achieved by oxygen/hydrogen treatment) preferred a hydrophilic NCD to adhesion. For this reason, more detailed characterization of osteoblast adhesion on NCD samples with hydrogen treatment (NCD-H, hydrophobic) and oxygen treatment (NCD-O, hydrophilic) on their entire surface was performed simultaneously to the experiments described in Publication C.

Since cell reactions to underlying substrate are mediated by protein layer formed between substrate and cells, we wondered whether some FBS proteins bind preferentially to NCD-O in comparison to NCD-H or vice versa. Since it is generally known that specific proteins are bound by specific integrins in cell membrane (83), we decided to focus on involvement of specific integrins in osteoblast adhesion to NCD-O and NCD-H. We choose integrin α5β1 (known as receptor for fibronectin) (159) and integrin αVβ5 (known as receptor for vitronectin) (160) as fibronectin and vitronectin are the best known adhesion proteins contained in the serum. For this purpose, inhibition of integrin α5β1 or αVβ5 in osteoblasts by antibodies was performed after series of optimization experiments. Osteoblasts with inhibition antibodies anti-integrin α5β1 or αVβ5 were seeded onto NCD-O and NCD-H and after 2 h, cell number and cell area were assessed in comparison to control without inhibition antibody.

The results (Figure 6) showed that no statistically significant differences were observed between numbers of cells adhered on NCD-H or NCD-O with inhibition of integrin α5β1 or αVβ5 in comparison to a control without inhibition antibody. This is caused by relatively large variance of measured values. However, statistically significantly lower amount of cells adhered on NCD-H with inhibited integrin α5β1 (62%) compared to number of cells adhered to NCD-O with inhibited integrin α5β1 (89%). On the other hand, lower amount of cells (but not statistically significantly) adhered on NCD-O with inhibited integrin αVβ5 (48%) compared to number of cells adhered to NCD-H with inhibited integrin αVβ5 (78%).

It seems that osteoblasts use the fibronectin receptor (integrin α5β1) to a larger extent for adhesion to hydrophobic NCD-H than to hydrophilic NCD-O. In contrast,

osteoblasts probably employ the vitronectin receptor (integrin αVβ5) more for adhesion to hydrophilic NCD-O than to hydrophobic NCD-H.

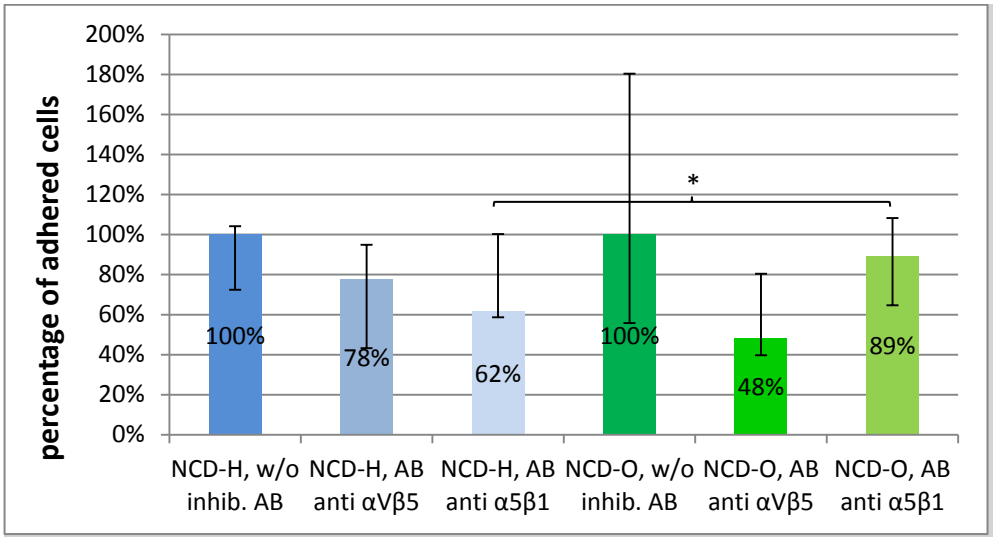

Figure 6: Cell number of osteoblasts cultivated after inhibiton of integrin αVβ5 or α5β1 on NCD-H and NCD-O surfaces for 2 h (N=10 fields of view). Medians with interquartile ranges are expressed. * - statistically significant difference at $p < 0.05$

For cell area (Figure 7), no statistically significant differences were observed between cell areas of cells adhered on NCD-H or NCD-O with inhibition of integrin α5β1 or αVβ5 in comparison to a control without inhibition antibody. However, smaller cell area (approximately 75 %) was detected in cells with inhibited integrin αVβ5 (vitronectin receptor) on both NCD-H and NCD-O compared to control. We could conclude that vitronectin promotes osteoblast spreading on both NCD-H and NCD-O.

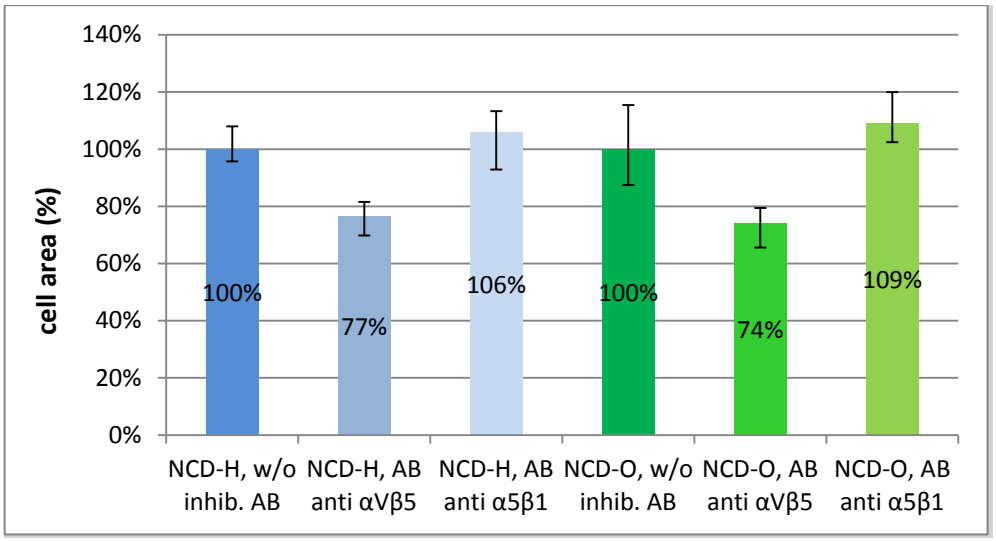

Figure 7: Cell area of osteoblasts cultivated after inhibiton of integrin αVβ5 or α5β1 on NCD-H and NCD-O surfaces for 2 h (N=10 fields of view). Medians with interquartile ranges are expressed.

Quantitative Polymerase Chain Reaction with Reverse Transcription (qRT-PCR) was used as a next method for more detailed characterization of osteoblast adhesion on NCD-H and NCD-O with respect to the presence or the absence of FBS. Osteoblasts were seeded on NCD-H, NCD-O and TCPS as a control in the presence and the absence of FBS (Table 2). After 2 h, RNA was isolated from all the tested samples and transcribed into cDNA using reverse transcriptase. Afterwards, quantitative PCR was performed with primers for various integrin subunits – α1, α2, α3, α5, αV, β1, β3 and β5 (Table 3).

Osteoblasts cultivated on TCPS for 2 h		Osteoblasts cultivated on NCD-H for 2 h		Osteoblasts cultivated on NCD-O for 2 h	
with FBS	without FBS	with FBS	without FBS	with FBS	without FBS

Table 2: Samples that were subjected to qRT-PCR analyses. RNA was isolated from these samples.

investigated α integrin subunits	α1, α2, α3, α5, αV
investigated β integrin subunits	β1, β3, β5

Table 3: **Investigated α and β subunits of integrin receptors.**

Integrin receptors are heterodimers composed of two subunits (α and β) and many (but not all) combinations of α and β subunits exist. For this reason, the expression of various individual α and β integrin subunits (Tab. 3) were investigated. Since integrin receptors work as dimers (α and β subunits together), the known combinations of tested integrin subunits is presented here as a result of performed experiments (Table 4).

The results (Table 4) are derived from three independent experiments that were performed in tetraplicates. Only the same result acquired in at least two experiments from three was considered as relevant. Expression level of tested integrin subunits was normalized to osteoblasts those were cultivated on TCPS with FBS (standard, calibrator). No tested integrins (both subunits) were up-regulated on NCD substrates compared to TCPS in the presence of FBS. Integrins α1β1 (collagen IV and laminin-1 receptor) and α2β1 (collagen and laminin receptor) were expressed at the same level in osteoblasts those adhered on NCD-O without FBS as in osteoblasts those adhered on TCPS with FBS. Integrins αVβ1 (vitronectin and fibronectin receptor) and αVβ3 (fibronectin, vitronectin, and thrombospondin receptor) were expressed at the same level in osteoblasts those adhered on NCD-H with FBS as in osteoblasts those adhered on TCPS with FBS.

Interestingly, integrin α5β5 (vitronectin receptor) was identically down-regulated in osteoblasts that adhered on NCD-H with and also without FBS compared to TCPS with FBS sample. Finally, integrins αVβ3 (fibronectin, vitronectin, and thrombospondin receptor) and αVβ5 (vitronectin receptor) were downregulated in osteoblasts that adhered on TCPS without FBS compared to TCPS with FBS.

For integrins α5β1 and αVβ5 that were investigated in previous section of this chapter (integrin inhibition by antibodies), no relevant expression profiles in cells those adhered on NCD-H and NCD-O were detected by qRT-PCR. It could be caused by different principles of both methods (adhesion with inhibited integrins by antibody and detection of RNA level of individual integrin subunits).

To conclude, it seems that osteoblasts those adhered on NCD-H do not prefer adhesion through vitronectin.

TCPS with FBS	TCPS without FBS	NCD-O with FBS	NCD-O without FBS	NCD-H with FBS	NCD-H without FBS
calibrator	αVβ3 (fibronectin, vitronectin, thrombospondin)	x	α1β1 (collagen IV and laminin-1)	αVβ1 (vitronectin and fibronectin)	α5β5 (vitronectin)
calibrator	αVβ5 (vitronectin)	x	α2β1 (collagen and laminin)	αVβ3 (fibronectin, vitronectin, thrombospondin)	x
calibrator	x	x	x	α5β5 (vitronectin)	x

Table 4: Summary of qRT-PCR results. Expression level of known combinations of integrin subunits in osteoblasts cultivated on NCD-O, NCD-H or TCPS in FBS presence (with FBS) or the absence (without FBS) normalized to TCPS with FBS. Gray color indicates the same expression level as TCPS with FBS. Blue color indicates down-regulation in comparison to TCPS with FBS. The empty boxes mean that no identical expression level of known combination of α and β integrin subunits were detected in at least two experiments. Known ligands of specific integrins are stated in brackets. This table is derived from 3 independent experiments that were done in tetraplicates.

To confirm these results, one pilot transcriptomic profiling experiment using microarray from Affymetrix was performed in collaboration with prof. Ondřej Šeda from Institute of Biology and Medical Genetics of the First Faculty of Medicine, Charles University in Prague and General University Hospital. This experiment was performed with osteoblasts seeded only on TCPS in the presence and the absence of FBS for 2 h. Unfortunately, no significant differences in integrin expression were detected by this method.

Taken together, we found out repeatedly that a cell adhesion in the absence of FBS differs extensively from a cell adhesion in FBS presence. For this reason, the effect of FBS on cell adhesion was further studied in more detail. Since these differences were observed regardless of used material, additional cell adhesion studies were performed only with TCPS. At first, effect of FBS proteins on osteoblast adhesion was

investigated. These results are presented in publication D that is under review in these days. Because of the effect of FBS proteins on cell adhesion could be cell type specific; this phenomenon was studied also with primary human fibroblasts and human mesenchymal stem cells (hMSCs). Since these results are not a part of the publication D, the results comparing effect of FBS on cell adhesion of all three above mentioned cell types will be presented in this thesis separately in a full form.

4.4 The effect of serum proteins on initial osteoblast adhesion on tissue culture polystyrene

4.4.1 Publication D: The effect of serum proteins on initial osteoblast adhesion

Martina Verdanova, Pavla Sauerova, Ute Hempel, Marie Hubalek Kalbacova (2016): The effect of serum proteins on initial osteoblast adhesion. Biochemistry and Cell Biology – submitted

This paper describes osteoblast adhesion on TCPS in the presence of FBS and in its absence 2 h after cell seeding. These two types of osteoblast adhesion differed a lot. More osteoblasts adhered on the TCPS surface in the absence of FBS proteins; these osteoblasts were larger, had a star-like shape and their adhesion strength was stronger (Fig. 2 in the enclosed Publication D). For more detailed characterization of osteoblast adhesion quality, the expression of the membrane protein CD44, signaling proteins (FAK, Rho, ERK 1/2), focal adhesion structural proteins (vinculin and talin) and actin cytoskeleton were studied by fluorescence microscopy. It was shown that no classic FAs were formed during osteoblast adhesion in FBS absence On the other hand, classic and similar to each other FAs were formed when 1%, 5% or 15% FBS was presented in medium (Fig. 1 in the enclosed Publication D). All studied signaling proteins (FAK, Rho and ERK 1/2) were expressed in a lesser extent in the osteoblasts those adhered without FBS proteins compared to the osteoblasts those adhered onto FBS proteins (Fig. 3 and 4 in the enclosed Publication D).

In order to evaluate the effect of the individual selected proteins originating from FBS on osteoblast adhesion, osteoblasts were seeded onto immobilized FN and VN for 2 h and 20 h. The osteoblasts that were cultivated on FN, VN and FBS exhibited comparable morphologies and FA patterns following a short period of cultivation (2 h); however, this similarity lessened after longer periods of cultivation (20 h). In contrast, the osteoblasts that were seeded and cultivated directly on the surface exhibited a morphology that differed significantly from the outset from those cells exposed to particular proteins. Moreover, no FAs were formed in FBS absence after 2 h, but big and pronounced FAs were produced in a few survived cells after 20 h (Fig. 5 and 6 in the enclosed Publication D).

4.4.2 Detailed characterization of initial osteoblast adhesion on tissue culture polystyrene depending on the presence and the absence of FBS

Moreover, we were interested in real-time monitoring of osteoblast adhesion in the presence and the absence of FBS by fluorescence microscopy. For these purposes, osteoblast cell line with stable expression of protein vinculin conjugated with GFP was prepared. For method optimization experiments, this stable cell line was seeded on glass surface (special surface for microscopy) in FBS presence and osteoblasts were monitored in real-time by fluorescence microscope for 48 h with increased imaging frequency during first 2 h.

Unfortunately, the optimization of this method failed despite series of optimization experiments with various set-ups and usage of a special heating chamber for monitoring of live cells by microscope. The biggest problem was early cell death caused by relatively frequent illumination of cells by blue laser and lower temperature in heating chamber. The other problem was a fast photobleaching of GFP.

For detailed characterization of osteoblast adhesion to TCPS in the presence and the absence of FBS after 2 h, one pilot transcriptomic profiling experiment using microarray from Affymetrix was performed in collaboration with prof. Ondřej Šeda. Many of transcripts (known and also unknown) showed changed expression in osteoblasts those adhered in FBS absence compared to osteoblasts those adhered in FBS presence. However, the most interesting result for us was the inhibition of ERK as an upstream driver that was predicted based on down-regulation of specific genes (Figure 8) in osteoblasts those adhered in FBS absence. Inhibition of cell proliferation was predicted as a corresponding downstream function. In addition, FAK was found as a protein having some relationship with down- and up-regulated genes in osteoblasts those adhered in FBS absence (Figure 9).

Taken together, these findings about ERK and FAK based on transcriptomic profiling corresponds with observations from immunofluorescence staining of proteins presented in Publication D (chapter 4.4.1).

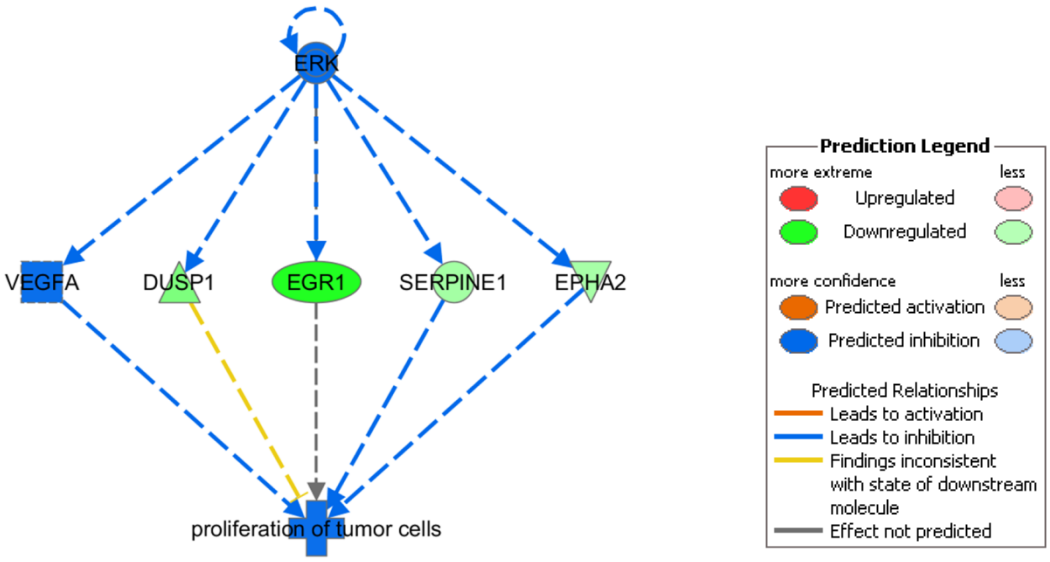

Figure 8: **Predicted effects of down-regulated genes in osteoblasts cultivated in FBS absence compared to the osteoblasts cultivated in FBS presence for 2 h** (generated by IPA software).

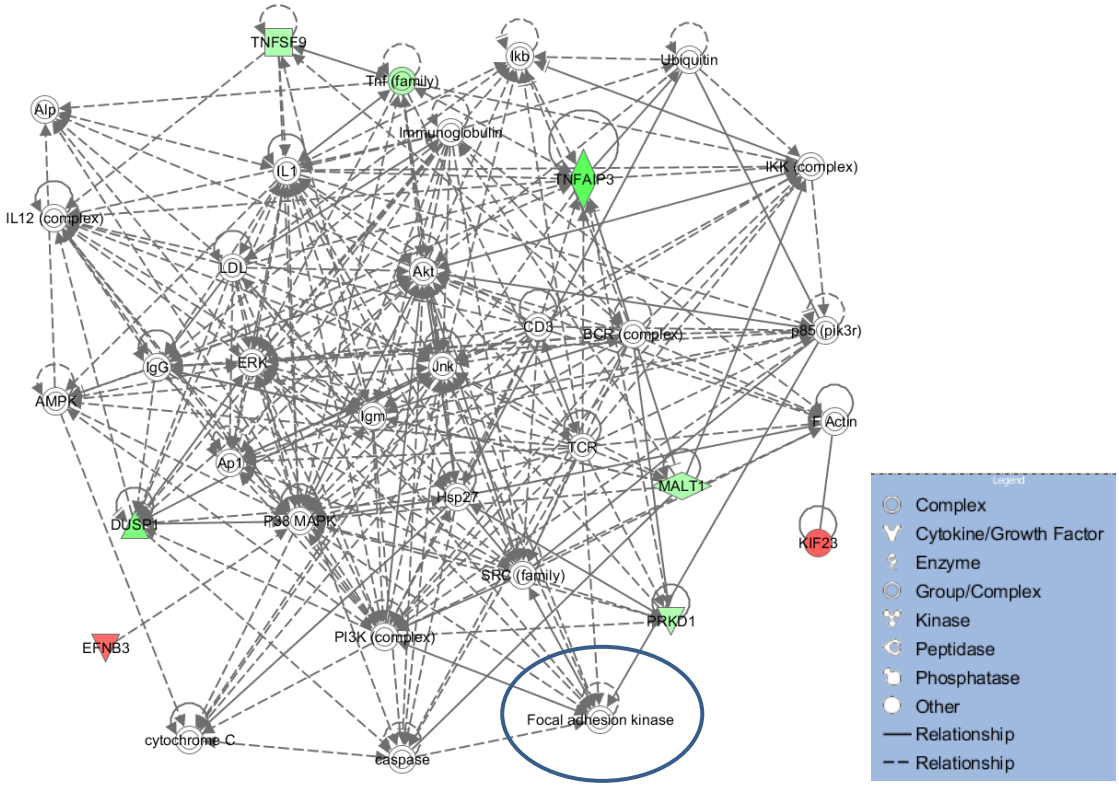

Figure 9: Network of affected genes in osteoblasts cultivated in FBS absence compared to the osteoblasts cultivated in FBS presence for 2 h (generated by IPA software).

Nevertheless, the Publication D showed that osteoblast adhesion mediated by FBS proteins differs extensively from the osteoblast adhesion without FBS protein contribution. The characterization of cell adhesion in the absence of FBS is necessary for many medical applications because of FBS cannot be used for clinical purposes. Study of "direct" cell adhesion to materials without contribution of proteins is important also for characterization of a pure interaction between cells and specific substrates. However, the effect of FBS on cell adhesion could be cell type specific. That is why the principal adhesion experiments were performed also with other cell types (primary human fibroblasts and hMSCs). The results comparing adhesion of osteoblasts, fibroblasts and hMSCs in the presence and the absence of FBS will be described in the next chapter in a full form.

4.5 Effect of FBS on initial adhesion of osteoblasts, fibroblasts and mesenchymal stem cells

Comparison of cell adhesion of human osteoblast-like cell line (SAOS-2), primary human fibroblasts and human mesenchymal stem cells (hMSCs) onto TCPS in the presence and the absence of FBS at 2 h after cell seeding was performed. Cell morphology of these cells is presented in Figure 10. Osteoblasts and hMSCs that adhered on FBS proteins had round shape in contrast to fibroblasts that had elongated and ragged shape. On the contrary, cell shape of osteoblasts and hMSCs that adhered on TCPS without FBS proteins had ragged shape and reversely fibroblasts had mostly round shape.

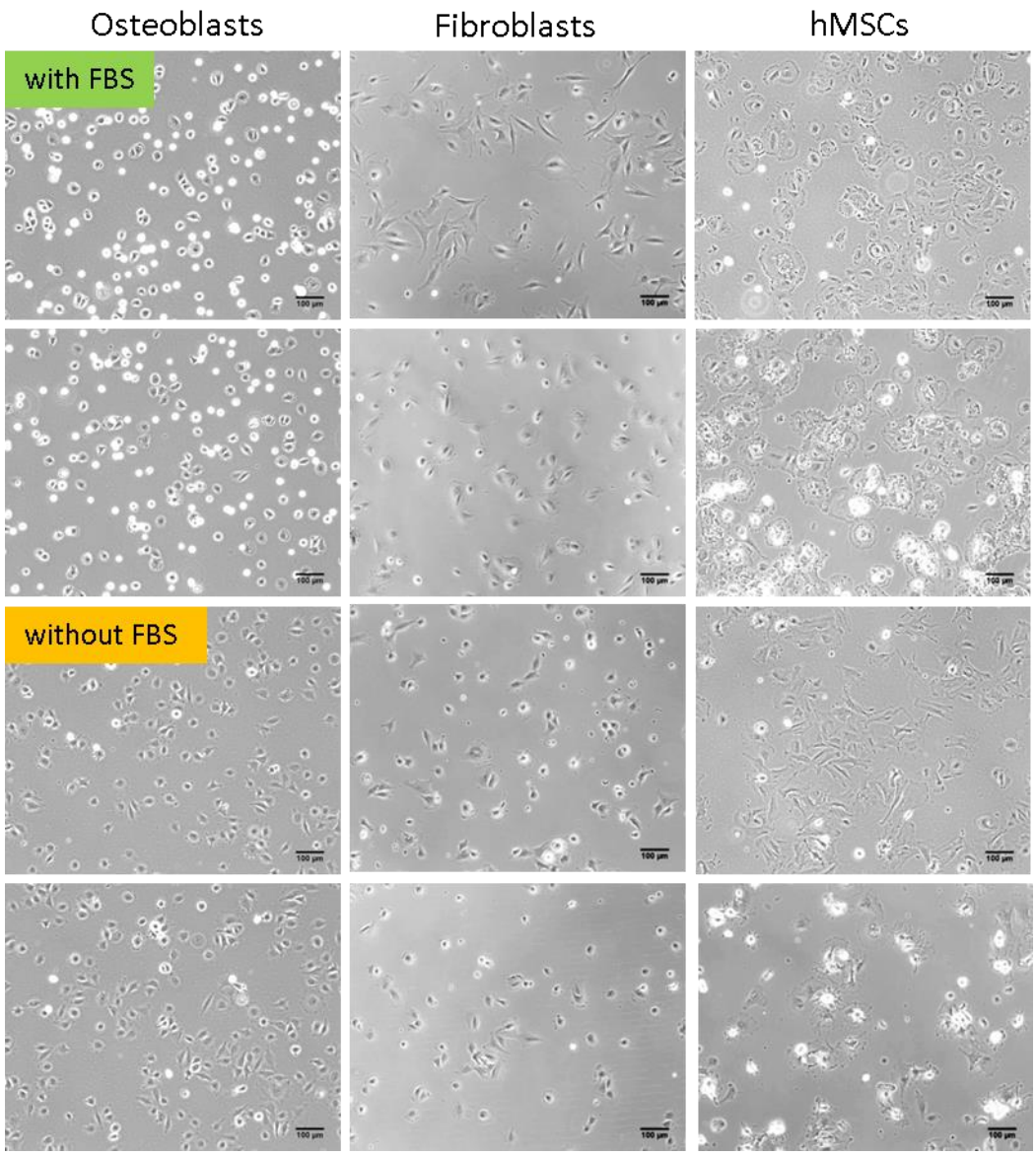

Figure 10: Phase contrast images of osteoblasts, fibroblasts and hMSCs that were cultivated with or without FBS for 2 h.

This observation correlates with measured cell area (Figure 11). Osteoblasts that adhered on FBS had smaller cell area than those adhered on TCPS without FBS proteins. The opposite state was found in fibroblasts. The similar cell area was observed in hMSCs that were seeded in FBS presence and absence. However, large variations were detected in cell area measurement of hMSCs.

As regards cell number, lower amount of osteoblasts was observed when cells adhered on TCPS in FBS presence than in FBS absence. The opposite situation was detected in fibroblasts and hMSCs where more cells was detected in FBS presence during cell seeding (Figure 12).

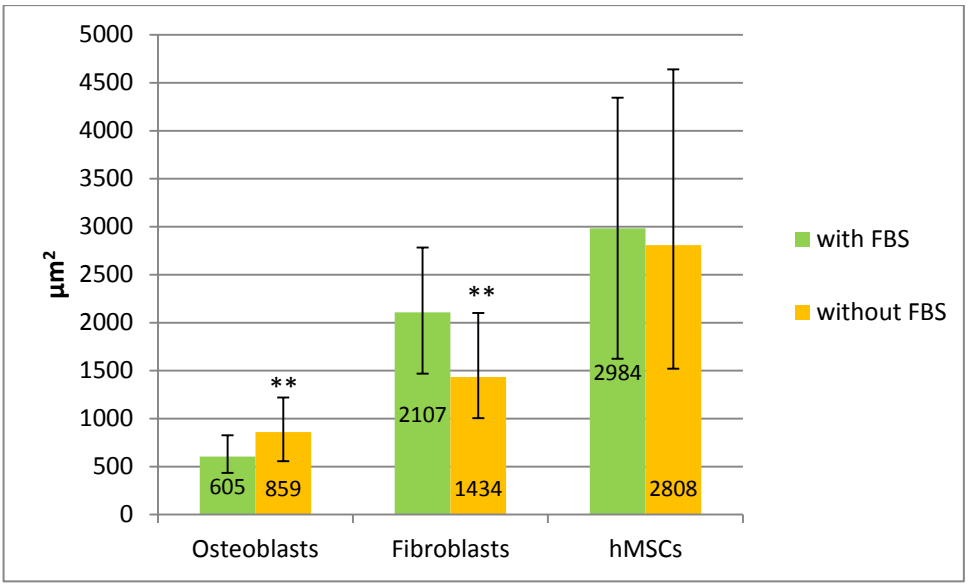

Figure 11: Cell area of osteoblasts (N=2000 cells), fibroblasts (N=450 cells) and hMSCs (N=250 cells) that were cultivated with or without FBS for 2 h. Medians with interquartile ranges are expressed. ** = $p < 0.001$, Mann-Whitney test (with vs. without FBS)

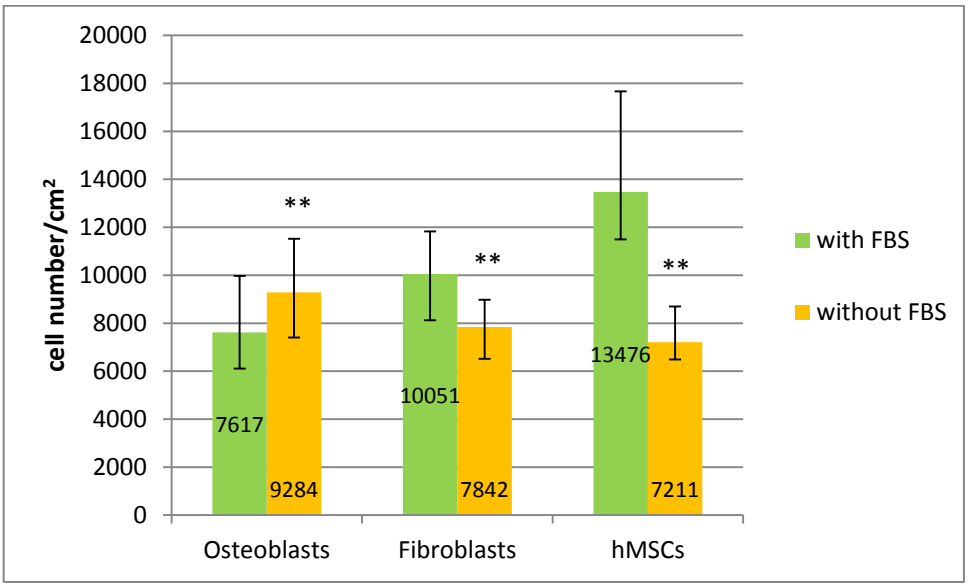

Figure 12: Cell number of osteoblasts (N=400 fields of view), fibroblasts (N=140 fields of view) and hMSCs (N=40 fields of view) that were cultivated with or without FBS for 2 h. Medians with interquartile ranges are expressed. ** = $p < 0.001$, Mann-Whitney test (with vs. without FBS)

To characterize a cell adhesion quality, the expression of proteins such as actin, vinculin, talin, CD44, pFAK, Rho and pERK1/2 in osteoblasts, fibroblasts and hMSCs that were cultivated with and without FBS for 2 h were studied by fluorescence microscopy (Figure 13).

A distribution of actin cytoskeleton was affected by a shape and morphology of cells. In the well-spread cells, actin signal revealed a filamentous character. On the other hand, actin ring on cell perimeter was observed in roundish cells.

Focal adhesion structural proteins vinculin and talin were localized in FAs in all three cell types that adhered in FBS presence in contrast to the cells that were seeded in FBS absence. The vinculin and actin signal in these cells was spread throughout whole cell with occasional intensification at the cell edges.

Membrane protein CD44 revealed diffuse signal with occasional aggregates irrespective of cell type and FBS presence.

Signaling protein pFAK showed the same expression pattern as vinculin or talin. pFAK was localized in FAs in all cells that adhered on TCPS in FBS presence and diffuse pFAK signal throughout whole cell with sporadic intensification at the cell edges was detected in all cells that adhered in FBS absence.

Signal of Rho GTPase was diffuse throughout whole cell with occasional intensification at the cell edges in osteoblasts and hMSCs that adhered on FBS proteins in contrast to fibroblasts where this expression pattern was observed rather in cells adhered in FBS absence. And vice versa, only diffuse signal of Rho protein was observed in osteoblasts and hMSCs that were seeded without FBS proteins and fibroblasts that adhered on FBS proteins. More of non-specific signal in cell surrounding was detected in all three cell types that adhered in FBS absence.

Signaling proteins pERK1/2 were localized at the cell edges in osteoblasts and hMSCs that adhered on FBS proteins. On the contrary, sporadic pERK1/2 signal at the cell edges but rather diffuse signal throughout whole cells was observed in osteoblasts and hMSCs that were seeded without FBS. In fibroblasts, pERK1/2 signal was distributed equally throughout whole cell with occasional intensification in the middle of cell and sometimes at the cell edges regardless of FBS presence.

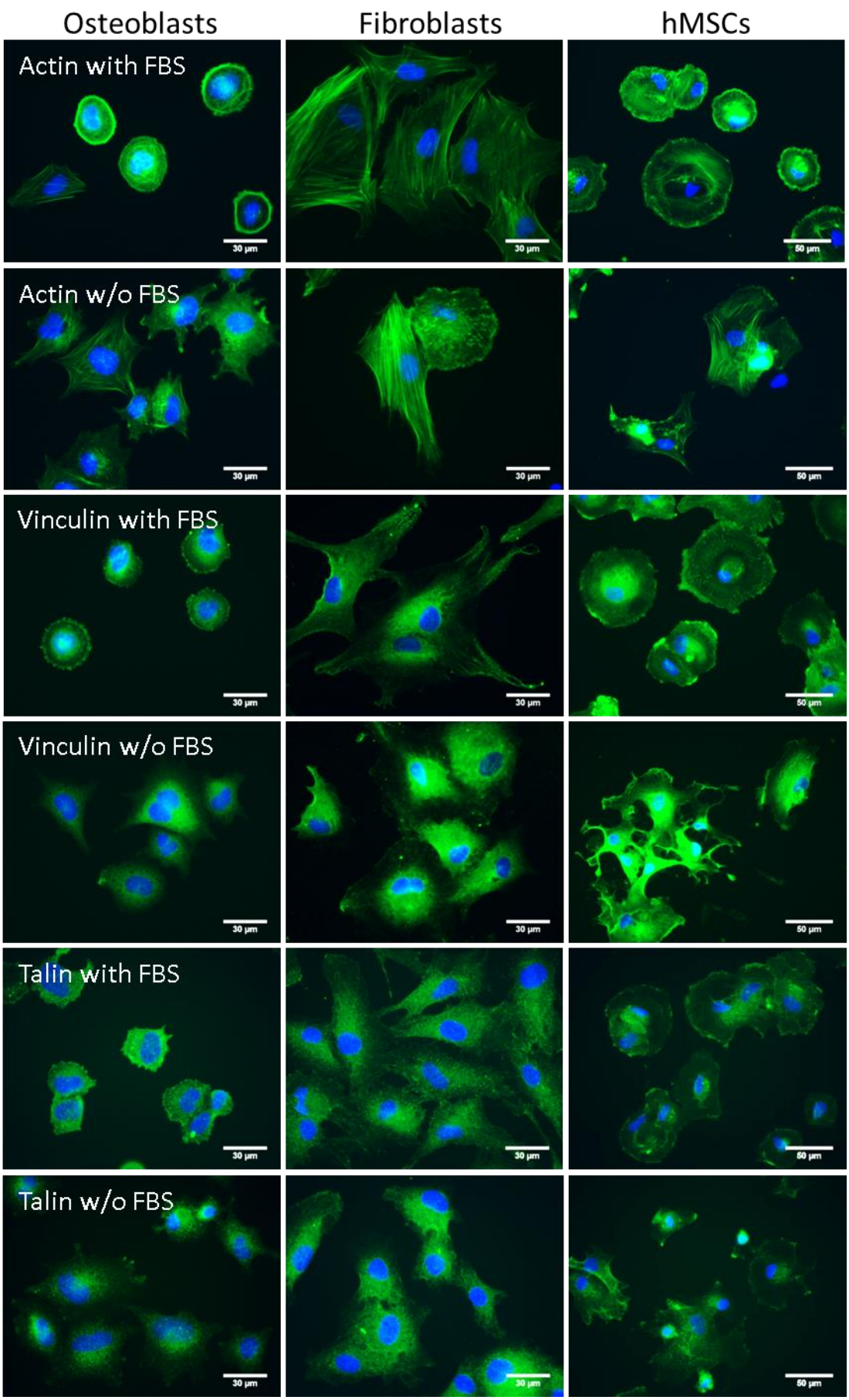
Osteoblasts
Fibroblasts
hMSCs
Actin with FBS
Actin w/o FBS
Vinculin with FBS
Vinculin w/o FBS
Talin with FBS
Talin w/o FBS
30 µm
50 µm

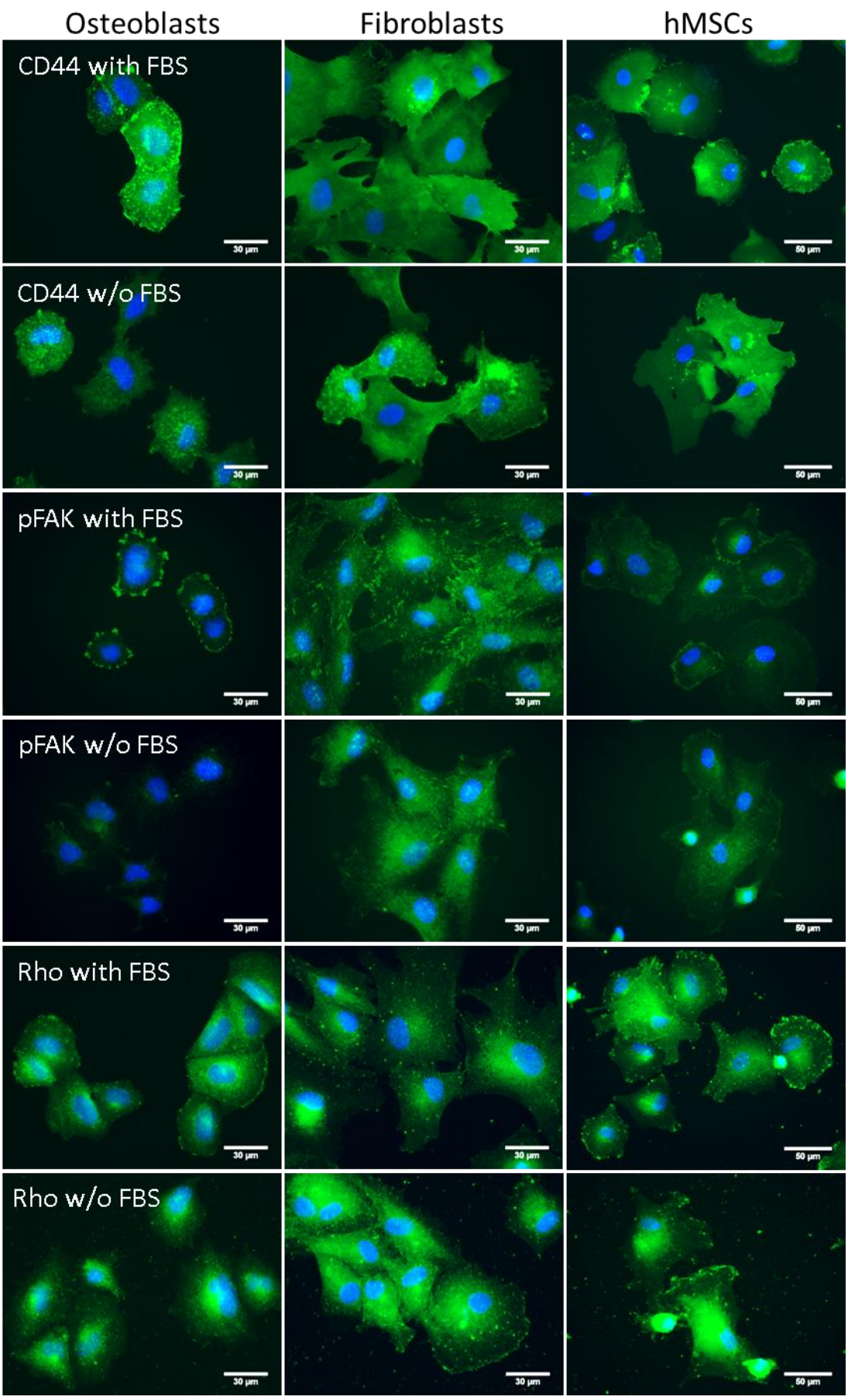
Osteoblasts
Fibroblasts
hMSCs
CD44 with FBS
CD44 w/o FBS
pFAK with FBS
pFAK w/o FBS
Rho with FBS
Rho w/o FBS
30 µm
50 µm

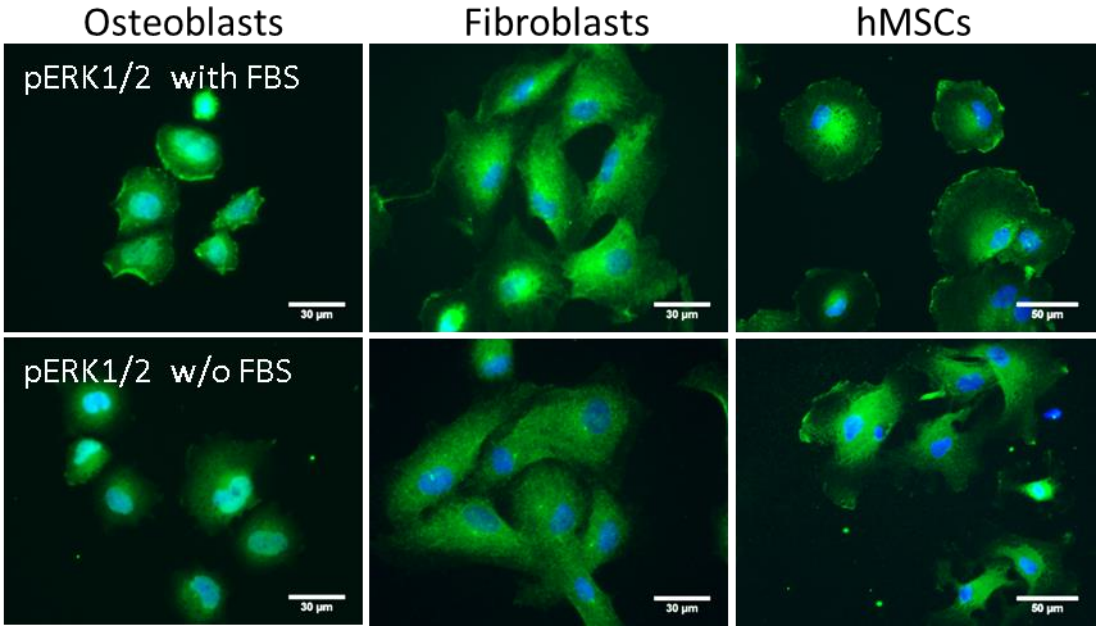

Figure 13: Effect of FBS on expression and localization of structural, membrane and signaling proteins in osteoblasts, fibroblasts and hMSCs that were cultivated with or without FBS for 2 h. Immunofluorescently stained proteins are depicted in the images.

Finally, osteoblasts and hMSCs demonstrated similar cell shape with respect to the presence of FBS. On the other hand, fibroblasts and hMSCs showed similar trend in cell number with regard to the presence of FBS. With regard to cell adhesion quality, all three cell types developed classic FAs with expression of vinculin, talin and pFAK in these FAs in contrast to all cells that were seeded without FBS that did not produce classic FAs. Osteoblasts and hMSCs differed slightly from fibroblasts only in localization of Rho and pERK1/2 proteins. It can be said that some features (especially cell shape, area and number) of cell adhesion considering the presence of FBS are cell type specific, but the mechanism of adhesion is similar for all the tested cell types.

4.6 Publication E: Evaluation of Sericin as a Fetal Bovine Serum-Replacing Cryoprotectant During Freezing of Human Mesenchymal Stromal Cells and Human Osteoblast-Like Cells

Martina Verdanova, Robert Pytlik, Marie Hubalek Kalbacova (2014): Evaluation of Sericin as a Fetal Bovine Serum-Replacing Cryoprotectant During Freezing of Human Mesenchymal Stromal Cells and Human Osteoblast-Like Cells. Biopreservation and Biobanking 12, 2, 99-105. $IF_{2014} = 1.340$

Since a freezing of cells is an essential method which researchers use during experimental work with cells, a study of use of various freezing media for two cell types commonly used in our laboratory was performed. For the reason that use of FBS in medical applications is problematic due to the danger of infection or allergic reaction, sericin was investigated as a replacement for FBS. Sericin is a sticky protein derived from the silkworm cocoon. Since DMSO is the most frequently used compound of freezing medium and its high concentrations are cytotoxic to eukaryotic cells (136, 141), DMSO-free or DMSO-low-concentration freezing media were also tested.

This paper compares various compositions of cryoprotective media (standard medium with 10% DMSO and 25% FBS; 1% and 5% sericin alone or in combination with 1%, 5% and 10% DMSO; 1%, 5% and 10% DMSO alone; 25% FBS alone; culture medium alone and DMSO alone) for freezing of osteosarcoma cell line SAOS-2 and hMSCs.

Cell viability (24 h after thawing, both hMSC and osteoblasts) and colony-forming ability (2 weeks after thawing, only for hMSCs) were determined. It was found that 1% sericin can replace FBS when 10% DMSO is present in freezing medium for hMSCs. Suprisingly, hMSCs could be frozen also in 10% DMSO as a single component of a standard culture medium (Fig. 1 in the enclosed Publication E). On the contrary, sericin cannot compensate FBS presence in freezing medium of osteoblast cell line. Moreover, either culture medium with only 10% DMSO was not adequate freezing medium for this cell line (Fig. 3 in the enclosed Publication E). Any decrease in DMSO concentration led to significantly worse survival of both types of cells.

In conclusion, sericin can substitute for FBS in the freezing medium for primary hMSCs, but cannot substitute for DMSO.

5 DISCUSSION

The first part of this thesis (Publications A-C) is focused on behavior of human osteoblasts that were cultivated on large-scale graphene (G) and nanocrystalline diamond (NCD). These nanomaterials are carbon allotropes, i.e. G and NCD have chemically the same composition; however, the arrangement of carbon atoms is different. G and NCD are materials with an extraordinary combination of properties such as high mechanical strength, electrical and thermal conductivity, great optical properties, possibility of functionalization and a very high surface area to volume ratio (3, 4, 29). For these reasons, G and NCD could be advantageously used in electronics (161, 162); however, they have a great potential also in biomedical applications that overlaps with the scope of this thesis.

Variously modified G and NCD resulting in their diverse properties were investigated in this thesis. Two hydrophobic samples, i.e. graphene treated with hydrogen (1-LG) and NCD treated with hydrogen (NCD-H) and two hydrophilic samples, i.e. graphene treated with oxygen (1-LG-O) and NCD treated with oxygen (NCD-O) were researched. These four tested samples vary at least in the carbon atom arrangement (G and NCD), degree of wettability and nanotopography.

Besides detailed characterization of the tested nanomaterials, the differences in osteoblast behavior on these two types of G (1-LG and 1-LG-O) and two types of NCD (NCD-H and NCD-O) after short (2 h) and longer (48 h) cultivation was examined. In order to reveal a direct effect of the tested materials on osteoblast behavior, the cells were cultivated on the substrates also in the initial (2 h) absence of FBS. To compare osteoblast behavior on G and NCD to some standard substrate, tissue culture treated polystyrene (TCPS) was used as a control.

Bone implant coating or cellular sensors represent the possible applications of G and NCD within the scope of this thesis. The fundamental information about cell interactions with these materials is essential but it has been only little examined so far.

To simplify this quite complicated study with a lot of variables, the osteoblast behavior on G and NCD without other influences will be discussed at first.

The very important finding of these studies is accelerated osteoblast proliferation on G compared to NCD and TCPS. It is an interesting phenomenon if we take into account that both G and NCD have chemically very similar structure in their pure form (both nanomaterials are made of only carbon atoms); however, the arrangement of

carbon atoms is different that results in various cell reactions to G and NCD. On the other hand, it should be mentioned that the important difference between G and NCD is their diverse topography in nanometer range (G revealed RMS roughness about 5 - 9 nm whereas NCD showed about 20 nm) (163). Many studies reported that cell behavior such as cell morphology, migration, proliferation and differentiation is largely affected by micro- and nanosized surface features (164). Moreover, one study presented discovery that nanotopography differences even less than 5 nm can also affect cell adhesion (165). For these reasons, only little nanoscale differences could be the cause (or one of many causes) of the diverse osteoblast reactions to G and NCD that were presented in this thesis.

Second, the effect of the treatment (with oxygen or hydrogen) of G and NCD on osteoblast behavior in the presence of FBS was examined. It was observed that the enhanced osteoblast proliferation on G was caused mainly by 1-LG where cell proliferation was superior. Higher cell proliferation on G treated with hydrogen compared to G treated with oxygen was observed also in previous study with hMSCs (166). In our studies, cells on 1-LG-O multiplied also more than cells on both NCDs and TCPS. The proliferation rate was calculated as a ratio of cell number at 48 h to cell number at 2 h and could be loaded by overestimation because of smaller number of cells were observed on G compared to NCD at 2 h while similar cell number was detected on both materials after 48 h. Yet the relative comparison still holds: the 1-LG provides for approximately 50% higher rate of cell multiplication than NCD and control TCPS. Moreover, full cell confluency was not reached in either case and the values are thus not limited by saturation.

The reason for accelerated cell proliferation rate on 1-LG compared to 1-LG-O and both NCDs could be the difference in “nanoroughness”, in particular the wrinkled morphology of 1-LG in nanoscale which was reflected by measured skew and kurtosis values. The positive effects of sub-100 nm structural features on the cells were reported previously (167, 168). The mechanism behind this phenomenon is probably the fact that nanotopography of materials greatly enhances the surface area enabling a binding of specific proteins in particular amounts and conformations (169). Moreover, the cell membrane in contact with the nanostructured surface is exposed to various mechanical forces that can reorganize its components and specific ion channels can open which can lead in changes in cell behavior (164).

As regards NCD, no significant dependence of osteoblast adhesion and proliferation on different surface terminations (oxygen or hydrogen) of topographically identical NCDs was revealed. This is in contrast with another study where NCD samples with hydrophilic/hydrophobic stripes rather than a homogeneous surface were used (60). In this set-up, cells preferred a hydrophilic NCD-O to adhesion. It could be caused by the fact that many of hydrophilic/hydrophobic borders are present on the striped NCD and cells can choose where to adhere in contrast to NCD samples with the whole hydrophobic or whole hydrophilic surface. Moreover, the preference to hydrophilic NCD on striped sample was valid only for a lower cell seeding density.

On the other hand, statistically significantly lower amount of osteoblasts adhered on NCD-H (homogenous hydrophobic surface) compared to NCD-O (homogenous hydrophilic surface) when integrin α5β1 was inhibited by antibody. Integrin α5β1 is also called the classic fibronectin receptor (119). It seems that osteoblasts use this fibronectin receptor (integrin α5β1) to a larger extent for adhesion to hydrophobic NCD-H than to hydrophilic NCD-O. It could be speculated that more FN or in more accessible conformation could bind to hydrophobic NCD-H than to hydrophilic NCD-O. In a literature, some studies showed higher affinity of fibronectin to hydrophilic surfaces (170, 171). However, other papers presented increased binding of fibronectin to hydrophobic surfaces (172, 173). Thus, he fibronectin affinity to various surfaces probably depends on more factors – e.g. on a concentration of fibronectin or a presence of other proteins. Moreover, also other surface properties next to wettability affect protein adsorption, e.g. negatively charged fibronectin could bind to positively charged surfaces.

In addition, we showed that vitronectin probably mediates osteoblast adhesion (as regards number of adhered cells) to hydrophilic NCD-O more than to hydrophobic NCD-H. Moreover, vitronectin likely promotes osteoblast spreading on both NCD-H and NCD-O in contrast to fibronectin. This is in correlation with previous study that discovered vitronectin and called it as a serum spreading factor (174).

As regards expression profiles of various integrin subunits on NCD-O, NCD-H and TCPS in FBS presence and its absence based on qRT-PCR method, no common features for type of material or presence of FBS were observed. Except interesting finding that integrin α5β5 (vitronectin receptor) is down-regulated in osteoblasts those adhered on NCD-H regardless of FBS presence compared to TCPS with FBS. This confirms the observation from inhibition of integrins by antibodies that showed

osteoblasts bind to NCD-H through fibronectin rather than vitronectin. It is interesting that no up-regulated genes were detected in osteoblasts cultivated on any NCD surface compared to those adhered on TCPS with FBS. Therefore, TCPS with FBS is probably a good standard for osteoblast adhesion in which various integrins are expressed at relatively high levels. However, we should keep in mind, that if DNA is transcribed it does not always mean that the RNA is translated. Moreover, a research of integrins is quite complicated since each type of integrin (a specific combination of α and β subunits) can bind more types of ligands and vice versa also one kind of ligand could be bound by several kinds of integrins (83).

The last point of view on osteoblast behavior on G and NCD is the presence or the absence of FBS during the first 2 h of cultivation that enable us to reveal the possible role of FBS proteins in cell-material interactions. After 2 h of cultivation in FBS absence, comparable numbers of cells were observed on all the tested substrates that are in contrast to standard conditions (FBS presence) where cell number on G, NCD and TCPS varied. This fact suggests that those cells in direct contact with the material sense its properties (topography, wettability and chemistry) to a lesser extent than the cells adhered on substrates through FBS proteins. Or the cells that adhered in FBS absence sense the surface properties similarly as the cells that adhered in the presence of FBS proteins, but the various cell reactions were not detected by techniques used in this thesis. In any case, our findings support the hypothesis that cell adhesion is substrate-dependent predominantly in the presence of FBS in the culture medium and that the selectivity of cell adhesion on various substrates is determined mainly through the selectivity of protein adsorption on particular substrates (175).

It was observed that FBS absence promoted cell adhesion on all the tested samples; however, subsequent cell proliferation was decreased despite FBS was added to cells for additional 46 h of cultivation. It seems that FBS somehow inhibited initial osteoblast adhesion. This phenomenon has previously also been reported for Jurkat cells (176). For this FBS-mediated inhibition of adhesion is probably responsible BSA (an abundant protein of FBS (177)) that inhibits cell spreading and functions as a repellent of cell adhesion (175, 178). Interestingly, the initial adhesion advantage (more cells) in FBS absence was followed by decreased cell proliferation during the time despite the addition of FBS. It is possible that cell adhesion in FBS absence is better in a quantitative point of view but not in a qualitative one. It means that cells in FBS

absence might not adhere effectively that could affect the subsequent cell proliferation negatively.

The enhanced osteoblast proliferation on 1-LG was detected also in the initial FBS absence. Thus, the factor behind this superior proliferation rate on 1-LG cannot only be protein interactions with surface nanotopography. However, the accelerated cell proliferation on 1-LG is clearly visible under both conditions – in FBS presence and absence. This is a great advantage for the potential use of 1-LG as a bioelectronic sensor and actuator where protein interlayers (layers between cells and electrode surface) can cause electrode fouling and affect sensor performance (179).

The next part of this thesis (including Publication D) is focused on differences between cell adhesion mediated by FBS proteins and cell adhesion without FBS proteins. To exclude cell type specific reactions, the major experiments were performed with human osteosarcoma cell line SAOS-2, hMSCs and primary human fibroblasts. A greater number of osteoblasts (SAOS-2) with a larger cell area were found on TCPS without FBS than with FBS. The opposite trend was observed with primary fibroblasts where higher number of larger cells was detected on TCPS with FBS compared to substrate without FBS. hMSCs revealed the same trend in cell number as primary fibroblasts. As regards cell area, hMSCs showed no significant difference between cell adhesion in FBS presence and absence; however, the interquartile ranges are high.

These different cell reactions are probably connected to the origin of cells. SAOS-2 cells are osteosarcoma cell line that is generaly used as a permanent line of human osteoblast-like cells (180). Osteoblast cancer cell line possesses some characteristic features (181) that can differ from features of primary and healthy cells such as primary human dermal fibroblasts and hMSCs. In a literature, a different adhesion of melanoma and fibroblastic cells to fibronectin was observed (182). It was shown that particular cell type could be able to bind only some specific adhesion motifs due to the exclusivity of interaction between cell surface adhesion receptors and particular adhesion motifs in proteins (183). Generally, tumor cells are characterized by changes in intercellular adhesion selectivity and also adhesion selectivity to ECM. Shifts in cell-cell and cell-ECM interactions (e.g. down- or up-regulation of integrin genes) are oncogene- and cell type-specific. However, cell adhesiveness is mostly reduced in cancer cells (184). This could explain the lower adhesiveness of osteosarcoma cell line in the presence of FBS in contrast to primary fibroblasts and

hMSCs from healthy donors, since FBS mimics the situation in the body where proteins are present.

The expression and especially localization of studied cell structural and signaling proteins varied significantly in cells that adhered on FBS proteins and those that adhered directly on the surface without FBS proteins. However, these differences were similar in all three studied cell types. Generally, the expression of particular proteins was largely affected by the cell morphology rather than by the specific cell type.

The most distinct feature was no formation of classic FAs in cells that adhered in FBS absence. The cells that adhere without any external proteins probably use a different mechanism to anchor themselves to the surface. This contact is probably mediated by non-specific physical interactions such as van der Waals bonding, hydrogen bonding or charged interactions between polar groups (e.g., hydroxyl) on the substrate and integrins on the cell surface (176).

Based on expression and localization of signaling proteins such as Rho, pFAK and ERK1/2, it could be said, that cell signaling in the absence of FBS is transduced by an alternative signaling pathway compared to the standard cell signaling initiated by FBS proteins (185). This hypothesis is supported by results obtained by two methods – transcriptomic profiling and immunofluorescence staining of proteins. Since a cell environment without FBS is poor in growth factors, a decreased level of activated, i.e. phosphorylated ERK1/2 was found in cells that adhered in FBS absence in contrast to the cells that adhered on FBS proteins. This is in correlation with the study by Chen *et al.* showing that the addition of growth factors to serum-deprived cells led to the increased phosphorylation of ERK proteins (186).

Osteoblasts were also cultivated for a longer time (20 h). Despite no FAs were formed after 2 h in FBS absence, FAs were produced after 20 h in those few survived cells. This could be caused by formation of an own cell-derived ECM; however, the exact time at which ECM production begins is unknown. The only information discovered in literature refers to few days (81). However, the most of osteoblasts that were cultivated in FBS absence for 20 h died in contrast to the cells that adhered on VN or FN own. This experiment confirmed the necessity of proper cell adhesion (mediated by FAs) for longer cultivation of anchorage-dependent cells.

The last part of this thesis (Publication E) concerns with evaluation of sericin as a replacement for FBS in freezing media for osteosarcoma cell line SAOS-2 and hMSCs. It was confirmed that DMSO is necessary for freezing of immortalized osteoblasts and also primary hMSCs and that the optimal DMSO concentration is 10%. This is in agreement with Baust et al. who demonstrated that 10% DMSO is the best concentration for fibroblasts, keratinocytes, hepatic and renal cells (187). This study showed that 1% sericin could substitute for 25% FBS in the freezing solution for primary hMSCs. Similar results were also published for rat insulinoma cell line, mouse hybridoma cell line (188) and for rat pancreatic islets (189). The novelty of our findings is that hMSCs could be cryopreserved in a growth medium containing only 10% DMSO without any additional proteins (FBS or sericin) with satisfactory results. Interestingly, freezing medium with 1% sericin instead of 25% FBS or medium containing only 10% DMSO was not beneficial for osteoblastic cell line.

It seems that primary hMSCs are more resistant to a heat stress (freezing and thawing) than the immortalized osteosarcoma cell line. A possible explanation could be the fact that hMSCs are less differentiated cells with more self-renewing ability compared to differentiated osteoblasts.

6 CONCLUSIONS

I. We characterized osteoblast behavior on differently treated graphene (G) and nanocrystalline diamond (NCD) in terms of cell adhesion and proliferation. Generally, both G and NCD exhibited better properties for osteoblast cultivation in comparison to control tissue culture polystyrene. Better cell adhesion but lower cell proliferation were observed on NCD compared to G. It was shown that osteoblasts adhered to hydrophobic NCD-H mainly through fibronectin, while they adhered to hydrophilic NCD-O predominantly through vitronectin. However, different wettability properties of topographically identical NCDs had no effect on osteoblast proliferation. In contrast, hydrophobic 1-LG with nanowrinkled topography enhanced cell proliferation extensively, in comparison to hydrophilic and flat 1-LG-O. Promoted cell proliferation enables faster cell colonization of G and NCD substrates, meaning faster new tissue formation which is beneficial in biomedical applications. Furthermore, it was shown that osteoblast adhesion was promoted in the initial absence of FBS; however, osteoblast proliferation was suppressed by these conditions.

II. We characterized cell adhesion of osteosarcoma cell line SAOS-2, primary human fibroblasts and human mesenchymal stem cells (hMSCs) in the presence and absence of FBS. For all three tested cell types, it was found that no classic focal adhesions were formed during cell adhesion in the absence of FBS proteins. Moreover, signaling within these cells proceeded in an unusual manner. In contrast, tested cell types differed in cell shape, area and number considering the adhesion in the presence or the absence of FBS. For the first time, the cell-substrate contact in the absence of serum proteins for anchorage-dependent cells was described in detail.

III. We evaluated the use of sericin as a replacement for FBS in freezing medium for osteosarcoma cell line and primary hMSCs from healthy donors. It was shown that 1 % sericin could substitute for 25 % FBS in the freezing medium for primary hMSCs in contrast to osteosarcoma cell line. Moreover, hMSCs could be cryopreserved in a growth medium containing only 10 % DMSO, with adequate results. Finally, different freezing formulas should be evaluated for different cell types to find the most satisfactory results.

7 COMPLETE LIST OF MY PUBLICATIONS

Martina Verdanova, Antonin Broz, Martin Kalbac, Marie Kalbacova (2012): Influence of oxygen and hydrogen treated graphene on cell adhesion in the presence or absence of fetal bovine serum. Phys. Status Solidi B 249, 12, 2503–2506. IF_{2012} = 1.489

Marie Hubalek Kalbacova, **Martina Verdanova**, Antonin Broz, Aliaksei Vetushka, Antonin Fejfar, Martin Kalbac (2014): Modulated surface of single-layer graphene controls cell behavior. Carbon 72, 207-214. IF_{2014} = 6.196

Martina Verdanova, Robert Pytlik, Marie Hubalek Kalbacova (2014): Evaluation of Sericin as a Fetal Bovine Serum-Replacing Cryoprotectant During Freezing of Human Mesenchymal Stromal Cells and Human Osteoblast-Like Cells. Biopreservation and Biobanking 12, 2, 99-105. IF_{2014} = 1.340

Marie Kalbáčová, **Martina Verdánová**, Filip Mravec, Tereza Halasová, Miloslav Pekař (2014): Effect of CTAB and CTAB in the presence of hyaluronan on selected human cell types. Colloids and Surfaces A: Physicochem. Eng. Aspects 460, 204–208. IF_{2014} = 2.752

Tomáš Suchý, Monika Šupová, Pavla Sauerová, **Martina Verdánová**, Zbyněk Sucharda, Šárka Rýglová, Margit Žaloudková, Radek Sedláček, Marie Hubálek Kalbáčová (2015): The effects of different cross-linking conditions on collagen-based nanocomposite scaffolds - an in vitro evaluation using mesenchymal stem cells. Biomed. Mater. 10, 065008. IF_{2014} = 3.697

Pavla Sauerová, **Martina Verdánová**, Filip Mravec, Tereza Pilgrová, Tereza Venerová, Marie Hubálek Kalbáčová, Miloslav Pekař (2015): Hyaluronic acid as a modulator of the cytotoxic effects of cationic surfactants. Colloids and Surfaces A: Physicochem. Eng. Aspects 483, 155–161. IF_{2014} = 2.752

Martina Verdanova, Bohuslav Rezek, Antonin Broz, Egor Ukraintsev, Oleg Babchenko, Anna Artemenko, Tibor Izak, Alexander Kromka, Martin Kalbac, Marie Hubalek Kalbacova (2016): Nanocarbon Allotropes - Graphene and Nanocrystalline Diamond - Promote Cell Proliferation. Small 12, 18, 2499–2509. IF_{2014} = 8.368

8 LIST OF ABBREVIATIONS

1-LG	single-layer graphene treated with H_2/Ar
1-LG-O	single-layer graphene treated in an oxidizing atmosphere
AFM	atomic force microscopy
ANOVA	analysis of variance
BSA	bovine serum albumin
CA	contact angle
cDNA	complementary deoxyribonucleic acid
CFU-F	colony-forming unit-fibroblast
Ct	cycle threshold
CVD	chemical vapor deposition
DAPI	4',6-diamidino-2-phenylindole
DMSO	dimethyl sulfoxide
DNA	deoxyribonucleic acid
ECM	extracellular matrix
ERK1/2	extracellular signal-regulated kinases 1 and 2
FA	focal adhesion
FAK	focal adhesion kinase
FBS	fetal bovine serum
FN	fibronectin
G	graphene
GAPDH	glyceraldehyde-3-phosphate dehydrogenase
GFOGER	glycine-phenylalanine-hydroxyprolin-glycine-glutamic acid-arginine
GFP	green fluorescent protein
GO	graphene oxide
GTP	guanosine-5'-triphosphate
HMBS	hydroxymethylbilane synthase
hMSCs	human mesenchymal stem cells
HPRT 1	hypoxanthine phosphoribosyltransferase 1
iPSC	induced pluripotent stem cell
LDV	leucine-aspartic acid-valine
MSC	mesenchymal stem cell
NCD	nanocrystalline diamond

NCD-H	NCD treated with hydrogen plasma
NCD-O	NCD treated with oxygen plasma
NHDF	normal human dermal fibroblasts
PCR	polymerase chain reaction
pERK1/2	phosphorylated extracellular signal-regulated kinases 1 and 2
pFAK	phosphorylated focal adhesion kinase
qPCR	quantitative polymerase chain reaction
qRT-PCR	quantitative polymerase chain reaction with reverse transcription
REDV	arginine-glutamic acid-aspartic acid-valine
RGD	arginin-glycin-aspartic acid
rGO	reduced graphene oxide
RMS	root mean square
RNA	ribonucleic acid
RT	room temperature
SAOS-2	sarcoma osteogenic cell line
SEM	scanning electron microscopy
TCPS	tissue culture polystyrene
VN	vitronectin
YIGSR	tyrosine-isoleucine-glycine-serine-arginine

9 REFERENCES

1. Padmanabhan J, Kyriakides TR. Nanomaterials, Inflammation, and Tissue Engineering. Wires Nanomed Nanobi. 2015;7(3):355-70.

2. Feng LZ, Liu ZA. Graphene in biomedicine: opportunities and challenges. Nanomedicine-Uk. 2011;6(2):317-24.

3. Cha C, Shin SR, Annabi N, Dokmeci MR, Khademhosseini A. Carbon-based nanomaterials: multifunctional materials for biomedical engineering. Acs Nano. 2013;7(4):2891-7.

4. Sanchez VC, Jachak A, Hurt RH, Kane AB. Biological Interactions of Graphene-Family Nanomaterials: An Interdisciplinary Review. Chem Res Toxicol. 2012;25(1):15-34.

5. 2016. Available from: http://www.nobelprize.org/nobel_prizes/physics/laureates/2010/.

6. Geim AK. Graphene: Status and Prospects. Science. 2009;324(5934):1530-4.

7. Mao HY, Laurent S, Chen W, Akhavan O, Imani M, Ashkarran AA, et al. Graphene: Promises, Facts, Opportunities, and Challenges in Nanomedicine. Chem Rev. 2013;113(5):3407-24.

8. Wang Y, Li Z, Wang J, Li J, Lin Y. Graphene and graphene oxide: biofunctionalization and applications in biotechnology. Trends Biotechnol. 2011;29(5):205-12.

9. Novoselov KS, Geim AK, Morozov SV, Jiang D, Zhang Y, Dubonos SV, et al. Electric field effect in atomically thin carbon films. Science. 2004;306(5696):666-9.

10. Zheng QB, Li ZG, Yang JH, Kim JK. Graphene oxide-based transparent conductive films. Prog Mater Sci. 2014;64:200-47.

11. Yamada T, Ishihara M, Kim J, Hasegawa M, Iijima S. A roll-to-roll microwave plasma chemical vapor deposition process for the production of 294 mm width graphene films at low temperature. Carbon. 2012;50(7):2615-9.

12. Yang M, Yao J, Duan YX. Graphene and its derivatives for cell biotechnology. The Analyst. 2013;138(1):72-86.

13. Dreyer DR, Park S, Bielawski CW, Ruoff RS. The chemistry of graphene oxide. Chem Soc Rev. 2010;39(1):228-40.

14. Shen H, Zhang LM, Liu M, Zhang ZJ. Biomedical Applications of Graphene. Theranostics. 2012;2(3):283-94.

15. Feng LZ, Zhang SA, Liu ZA. Graphene based gene transfection. Nanoscale. 2011;3(3):1252-7.

16. Liu Z, Robinson JT, Sun X, Dai H. PEGylated nanographene oxide for delivery of water-insoluble cancer drugs. Journal of the American Chemical Society. 2008;130(33):10876-7.

17. Pumera M. Graphene in biosensing. Mater Today. 2011;14(7-8):308-15.

18. Mei QS, Zhang K, Guan GJ, Liu BH, Wang SH, Zhang ZP. Highly efficient photoluminescent graphene oxide with tunable surface properties. Chem Commun. 2010;46(39):7319-21.

19. Liu S, Zeng TH, Hofmann M, Burcombe E, Wei J, Jiang R, et al. Antibacterial activity of graphite, graphite oxide, graphene oxide, and reduced graphene oxide: membrane and oxidative stress. Acs Nano. 2011;5(9):6971-80.

20. Song B, Zhang C, Zeng GM, Gong JL, Chang YN, Jiang Y. Antibacterial properties and mechanism of graphene oxide-silver nanocomposites as bactericidal agents for water disinfection. Archives of biochemistry and biophysics. 2016;604:167-76.

21. Kalbacova M, Broz A, Kong J, Kalbac M. Graphene substrates promote adherence of human osteoblasts and mesenchymal stromal cells. Carbon. 2010;48(15):4323-9.

22. Lee WC, Lim CHYX, Shi H, Tang LAL, Wang Y, Lim CT, et al. Origin of Enhanced Stem Cell Growth and Differentiation on Graphene and Graphene Oxide. Acs Nano. 2011;5(9):7334-41.

23. Alzhavan O, Ghaderi E, Shahsavar M. Graphene nanogrids for selective and fast osteogenic differentiation of human mesenchymal stem cells. Carbon. 2013;59:200-11.

24. Chen GY, Pang DWP, Hwang SM, Tuan HY, Hu YC. A graphene-based platform for induced pluripotent stem cells culture and differentiation. Biomaterials. 2012;33(2):418-27.

25. Lin F, Du F, Huang J, Chau A, Zhou Y, Duan H, et al. Substrate effect modulates adhesion and proliferation of fibroblast on graphene layer. Colloids and surfaces B, Biointerfaces. 2016;146:785-93.

26. Wang K, Ruan J, Song H, Zhang JL, Wo Y, Guo SW, et al. Biocompatibility of Graphene Oxide. Nanoscale Res Lett. 2011;6.

27. Chatterjee N, Eom HJ, Choi J. A systems toxicology approach to the surface functionality control of graphene-cell interactions. Biomaterials. 2014;35(4):1109-27.

28. Yang K, Wan J, Zhang S, Zhang Y, Lee ST, Liu Z. In vivo pharmacokinetics, long-term biodistribution, and toxicology of PEGylated graphene in mice. Acs Nano. 2011;5(1):516-22.
29. Schrand AM, Hens SAC, Shenderova OA. Nanodiamond Particles: Properties and Perspectives for Bioapplications. Crit Rev Solid State. 2009;34(1-2):18-74.
30. Tang L, Tsai C, Gerberich WW, Kruckeberg L, Kania DR. Biocompatibility of Chemical-Vapor-Deposited Diamond. Biomaterials. 1995;16(6):483-8.
31. Fries MD, Vohra YK. Properties of nanocrystalline diamond thin films grown by MPCVD for biomedical implant purposes. Diam Relat Mat. 2004;13(9):1740-3.
32. Kromka A, Babchenko O, Izak T, Hruska K, Rezek B. Linear antenna microwave plasma CVD deposition of diamond films over large areas. Vacuum. 2012;86(6):776-9.
33. Tsugawa K, Kawaki S, Ishihara M, Kim J, Koga Y, Sakakita H, et al. Nanocrystalline diamond growth in a surface-wave plasma. Diam Relat Mat. 2011;20(5-6):833-8.
34. Jiang X, Klages CP, Zachai R, Hartweg M, Fusser HJ. Epitaxial Diamond Thin-Films on (001) Silicon Substrates. Appl Phys Lett. 1993;62(26):3438-40.
35. Williams OA. Nanocrystalline diamond. Diam Relat Mat. 2011;20(5-6):621-40.
36. Szunerits S, Boukherroub R. Different strategies for functionalization of diamond surfaces. J Solid State Electr. 2008;12(10):1205-18.
37. Zhang XQ, Chen M, Lam R, Xu XY, Osawa E, Ho D. Polymer-Functionalized Nanodiamond Platforms as Vehicles for Gene Delivery. Acs Nano. 2009;3(9):2609-16.
38. Lien ZY, Hsu TC, Liu KK, Liao WS, Hwang KC, Chao JI. Cancer cell labeling and tracking using fluorescent and magnetic nanodiamond. Biomaterials. 2012;33(26):6172-85.
39. Izak T, Novotna K, Kopova I, Bacakova L, Rezek B, Kromka A. H-terminated diamond as optically transparent impedance sensor for real-time monitoring of cell growth. Phys Status Solidi B-Basic Solid State Phys. 2013;250(12):2741-6.
40. Yang L, Sheldon BW, Webster TJ. The impact of diamond nanocrystallinity on osteoblast functions. Biomaterials. 2009;30(20):3458-65.
41. Edgington RJ, Thalhammer A, Welch JO, Bongrain A, Bergonzo P, Scorsone E, et al. Patterned neuronal networks using nanodiamonds and the effect of varying nanodiamond properties on neuronal adhesion and outgrowth. Journal of neural engineering. 2013;10(5).

42. Rezek B, Michalikova L, Ukraintsev E, Kromka A, Kalbacova M. Micro-pattern guided adhesion of osteoblasts on diamond surfaces. Sensors (Basel). 2009;9(5):3549-62.

43. Liskova J, Babchenko O, Varga M, Kromka A, Hadraba D, Svindrych Z, et al. Osteogenic cell differentiation on H-terminated and O-terminated nanocrystalline diamond films. Int J Nanomedicine. 2015;10:869-84.

44. Chen YC, Lee DC, Hsiao CY, Chung YF, Chen HC, Thomas JP, et al. The effect of ultra-nanocrystalline diamond films on the proliferation and differentiation of neural stem cells. Biomaterials. 2009;30(20):3428-35.

45. Medina O, Nocua J, Mendoza F, Gomez-Moreno R, Avalos J, Rodriguez C, et al. Bactericide and bacterial anti-adhesive properties of the nanocrystalline diamond surface. Diam Relat Mat. 2012;22:77-81.

46. Jakubowski W, Bartosz G, Niedzielski P, Szymanski W, Walkowiak B. Nanocrystalline diamond surface is resistant to bacterial colonization. Diam Relat Mat. 2004;13(10):1761-3.

47. Fucikova A, Valenta J, Pelant I, Kalbacova MH, Broz A, Rezek B, et al. Silicon nanocrystals and nanodiamonds in live cells: photoluminescence characteristics, cytotoxicity and interaction with cell cytoskeleton. Rsc Adv. 2014;4(20):10334-42.

48. Zakrzewska KE, Samluk A, Wierzbicki M, Jaworski S, Kutwin M, Sawosz E, et al. Analysis of the cytotoxicity of carbon-based nanoparticles, diamond and graphite, in human glioblastoma and hepatoma cell lines. Plos One. 2015;10(3):e0122579.

49. Schrand AM, Huang H, Carlson C, Schlager JJ, Omacr Sawa E, Hussain SM, et al. Are diamond nanoparticles cytotoxic? The journal of physical chemistry B. 2007;111(1):2-7.

50. Kalbacova M, Kalbac M, Dunsch L, Kromka A, Vaněček M, Rezek B, et al. The effect of SWCNT and nano-diamond films on human osteoblast cells. physica status solidi (b). 2007;244(11):4356-9.

51. Amaral M, Gomes PS, Lopes MA, Santos JD, Silva RF, Fernandes MH. Nanocrystalline diamond as a coating for joint implants: cytotoxicity and biocompatibility assessment. J Nanomaterials. 2008;2008:1-9.

52. Anselme K. Biomaterials and interface with bone. Osteoporos Int. 2011;22(6):2037-42.

53. Engler AJ, Sen S, Sweeney HL, Discher DE. Matrix elasticity directs stem cell lineage specification. Cell. 2006;126(4):677-89.

54. Förch R, Schönherr H, Jenkins ATA. Surface Design: Applications in Bioscience and Nanotechnology: Wiley; 2009.

55. Wei JH, Igarashi T, Okumori N, Igarashi T, Maetani T, Liu BL, et al. Influence of surface wettability on competitive protein adsorption and initial attachment of osteoblasts. Biomed Mater. 2009;4(4).

56. Denis FA, Hanarp P, Sutherland DS, Gold J, Mustin C, Rouxhet PG, et al. Protein adsorption on model surfaces with controlled nanotopography and chemistry. Langmuir. 2002;18(3):819-28.

57. Valamehr B, Jonas SJ, Polleux J, Qiao R, Guo SL, Gschweng EH, et al. Hydrophobic surfaces for enhanced differentiation of embryonic stem cell-derived embryoid bodies. P Natl Acad Sci USA. 2008;105(38):14459-64.

58. Chen GY, Pang DW, Hwang SM, Tuan HY, Hu YC. A graphene-based platform for induced pluripotent stem cells culture and differentiation. Biomaterials. 2012;33(2):418-27.

59. Lechleitner T, Klauser F, Seppi T, Lechner J, Jennings P, Perco P, et al. The surface properties of nanocrystalline diamond and nanoparticulate diamond powder and their suitability as cell growth support surfaces. Biomaterials. 2008;29(32):4275-84.

60. Rezek B, Michalikova L, Ukraintsev E, Kromka A, Kalbacova M. Micro-Pattern Guided Adhesion of Osteoblasts on Diamond Surfaces. Sensors-Basel. 2009;9(5):3549-62.

61. Zinger O, Anselme K, Denzer A, Habersetzer P, Wieland M, Jeanfils J, et al. Time-dependent morphology and adhesion of osteoblastic cells on titanium model surfaces featuring scale-resolved topography. Biomaterials. 2004;25(14):2695-711.

62. Gentile F, Tirinato L, Battista E, Causa F, Liberale C, di Fabrizio EM, et al. Cells preferentially grow on rough substrates. Biomaterials. 2010;31(28):7205-12.

63. Gill ST, Hinnefeld JH, Zhu SZ, Swanson WJ, Li T, Mason N. Mechanical Control of Graphene on Engineered Pyramidal Strain Arrays. Acs Nano. 2015;9(6):5799-806.

64. Kalbacova M, Rezek B, Baresova V, Wolf-Brandstetter C, Kromka A. Nanoscale topography of nanocrystalline diamonds promotes differentiation of osteoblasts. Acta Biomater. 2009;5(8):3076-85.

65. Kalbacova M, Rezek B, Baresova V, Wolf-Brandstetter C, Kromka A. Nanoscale topography of nanocrystalline diamonds promotes differentiation of osteoblasts. Acta Biomater. 2009;5(8):3076-85.

66. Gittens RA, McLachlan T, Olivares-Navarrete R, Cai Y, Berner S, Tannenbaum R, et al. The effects of combined micron-/submicron-scale surface roughness and nanoscale features on cell proliferation and differentiation. Biomaterials. 2011;32(13):3395-403.

67. Ballo A, Agheli H, Lausmaa J, Thomsen P, Petronis S. Nanostructured model implants for in vivo studies: influence of well-defined nanotopography on de novo bone formation on titanium implants. Int J Nanomed. 2011;6:3415-28.

68. Hart A, Gadegaard N, Wilkinson CD, Oreffo RO, Dalby MJ. Osteoprogenitor response to low-adhesion nanotopographies originally fabricated by electron beam lithography. Journal of materials science Materials in medicine. 2007;18(6):1211-8.

69. Biggs MJ, Richards RG, Gadegaard N, Wilkinson CD, Dalby MJ. The effects of nanoscale pits on primary human osteoblast adhesion formation and cellular spreading. Journal of materials science Materials in medicine. 2007;18(2):399-404.

70. Dalby MJ, Gadegaard N, Tare R, Andar A, Riehle MO, Herzyk P, et al. The control of human mesenchymal cell differentiation using nanoscale symmetry and disorder. Nat Mater. 2007;6(12):997-1003.

71. Lih E, Oh SH, Joung YK, Lee JH, Han DK. Polymers for cell/tissue anti-adhesion. Progress in polymer science. 2015;44:28-61.

72. Schakenraad JM, Busscher HJ. Cell Polymer Interactions - the Influence of Protein Adsorption. Colloid Surface. 1989;42(3-4):331-43.

73. Hallab NJ, Bundy KJ, O'Connor K, Moses RL, Jacobs JJ. Evaluation of metallic and polymeric biomaterial surface energy and surface roughness characteristics for directed cell adhesion. Tissue Eng. 2001;7(1):55-71.

74. Schneider GB, English A, Abraham M, Zaharias R, Stanford C, Keller J. The effect of hydrogel charge density on cell attachment. Biomaterials. 2004;25(15):3023-8.

75. Jung H, Kwak B, Yang HS, Tae G, Kim JS, Shin K. Attachment of cells to poly(styrene-co-acrylic acid) thin films with various charge densities. Colloid Surface A. 2008;313:562-6.

76. Geiger B, Spatz JP, Bershadsky AD. Environmental sensing through focal adhesions. Nature reviews Molecular cell biology. 2009;10(1):21-33.

77. Berrier AL, Yamada KM. Cell-matrix adhesion. Journal of cellular physiology. 2007;213(3):565-73.

78. Geiger B, Yamada KM. Molecular Architecture and Function of Matrix Adhesions. Csh Perspect Biol. 2011;3(5).

79. Frisch SM, Francis H. Disruption of epithelial cell-matrix interactions induces apoptosis. J Cell Biol. 1994;124(4):619-26.

80. Chiarugi P, Giannoni E. Anoikis: a necessary death program for anchorage-dependent cells. Biochemical pharmacology. 2008;76(11):1352-64.

81. Anselme K, Ploux L, Ponche A. Cell/Material Interfaces: Influence of Surface Chemistry and Surface Topography on Cell Adhesion. J Adhes Sci Technol. 2010;24(5):831-52.

82. Hynes RO. Integrins: bidirectional, allosteric signaling machines. Cell. 2002;110(6):673-87.

83. Humphries JD, Byron A, Humphries MJ. Integrin ligands at a glance. J Cell Sci. 2006;119(Pt 19):3901-3.

84. Aplin AE, Howe A, Alahari SK, Juliano RL. Signal transduction and signal modulation by cell adhesion receptors: the role of integrins, cadherins, immunoglobulin-cell adhesion molecules, and selectins. Pharmacol Rev. 1998;50(2):197-263.

85. Moser M, Legate KR, Zent R, Fassler R. The tail of integrins, talin, and kindlins. Science. 2009;324(5929):895-9.

86. Valdembri D, Serini G. Regulation of adhesion site dynamics by integrin traffic. Current opinion in cell biology. 2012;24(5):582-91.

87. Legate KR, Wickstrom SA, Fassler R. Genetic and cell biological analysis of integrin outside-in signaling. Gene Dev. 2009;23(4):397-418.

88. Miyamoto S, Teramoto H, Gutkind JS, Yamada KM. Integrins can collaborate with growth factors for phosphorylation of receptor tyrosine kinases and MAP kinase activation: roles of integrin aggregation and occupancy of receptors. J Cell Biol. 1996;135(6 Pt 1):1633-42.

89. Ivaska J, Heino J. Cooperation between integrins and growth factor receptors in signaling and endocytosis. Annual review of cell and developmental biology. 2011;27:291-320.

90. Riveline D, Zamir E, Balaban NQ, Schwarz US, Ishizaki T, Narumiya S, et al. Focal contacts as mechanosensors: Externally applied local mechanical force induces growth of focal contacts by an mDia1-dependent and ROCK-independent mechanism. J Cell Biol. 2001;153(6):1175-85.

91. Di Paolo G, Pellegrini L, Letinic K, Cestra G, Zoncu R, Voronov S, et al. Recruitment and regulation of phosphatidylinositol phosphate kinase type 1 gamma by the FERM domain of talin. Nature. 2002;420(6911):85-9.

92. Grinnell F. Focal adhesion sites and the removal of substratum-bound fibronectin. J Cell Biol. 1986;103(6 Pt 2):2697-706.

93. Kanchanawong P, Shtengel G, Pasapera AM, Ramko EB, Davidson MW, Hess HF, et al. Nanoscale architecture of integrin-based cell adhesions. Nature. 2010;468(7323):580-4.

94. Humphries JD, Wang P, Streuli C, Geiger B, Humphries MJ, Ballestrem C. Vinculin controls focal adhesion formation by direct interactions with talin and actin. J Cell Biol. 2007;179(5):1043-57.

95. Izzard CS. A precursor of the focal contact in cultured fibroblasts. Cell motility and the cytoskeleton. 1988;10(1-2):137-42.

96. Zamir E, Katz M, Posen Y, Erez N, Yamada KM, Katz BZ, et al. Dynamics and segregation of cell-matrix adhesions in cultured fibroblasts. Nat Cell Biol. 2000;2(4):191-6.

97. Geiger B, Bershadsky A, Pankov R, Yamada KM. Transmembrane crosstalk between the extracellular matrix--cytoskeleton crosstalk. Nature reviews Molecular cell biology. 2001;2(11):793-805.

98. Carragher NO, Frame MC. Focal adhesion and actin dynamics: a place where kinases and proteases meet to promote invasion. Trends Cell Biol. 2004;14(5):241-9.

99. Winograd-Katz SE, Fassler R, Geiger B, Legate KR. The integrin adhesome: from genes and proteins to human disease. Nat Rev Mol Cell Bio. 2014;15(4):273-88.

100. Calderwood DA, Campbell ID, Critchley DR. Talins and kindlins: partners in integrin-mediated adhesion. Nature reviews Molecular cell biology. 2013;14(8):503-17.

101. Critchley DR. Biochemical and structural properties of the integrin-associated cytoskeletal protein talin. Annu Rev Biophys. 2009;38:235-54.

102. Saunders RM, Holt MR, Jennings L, Sutton DH, Barsukov IL, Bobkov A, et al. Role of vinculin in regulating focal adhesion turnover. Eur J Cell Biol. 2006;85(6):487-500.

103. Goldmann WH, Ingber DE. Intact vinculin protein is required for control of cell shape, cell mechanics, and rac-dependent lamellipodia formation. Biochem Bioph Res Co. 2002;290(2):749-55.

104. Case LB, Baird MA, Shtengel G, Campbell SL, Hess HF, Davidson MW, et al. Molecular mechanism of vinculin activation and nanoscale spatial organization in focal adhesions. Nat Cell Biol. 2015;17(7):880-92.
105. Schlaepfer DD, Hauck CR, Sieg DJ. Signaling through focal adhesion kinase. Progress in biophysics and molecular biology. 1999;71(3-4):435-78.
106. Parsons JT. Focal adhesion kinase: the first ten years. J Cell Sci. 2003;116(Pt 8):1409-16.
107. Mitra SK, Hanson DA, Schlaepfer DD. Focal adhesion kinase: In command and control of cell motility. Nat Rev Mol Cell Bio. 2005;6(1):56-68.
108. Etienne-Manneville S, Hall A. Rho GTPases in cell biology. Nature. 2002;420(6916):629-35.
109. Bustelo XR, Sauzeau V, Berenjeno IM. GTP-binding proteins of the Rho/Rac family: regulation, effectors and functions in vivo. Bioessays. 2007;29(4):356-70.
110. Roskoski R, Jr. ERK1/2 MAP kinases: structure, function, and regulation. Pharmacological research : the official journal of the Italian Pharmacological Society. 2012;66(2):105-43.
111. Yoon S, Seger R. The extracellular signal-regulated kinase: multiple substrates regulate diverse cellular functions. Growth factors. 2006;24(1):21-44.
112. Reitsma S, Slaaf DW, Vink H, van Zandvoort MA, oude Egbrink MG. The endothelial glycocalyx: composition, functions, and visualization. Pflugers Archiv : European journal of physiology. 2007;454(3):345-59.
113. Boettiger D, Wehrle-Haller B. Integrin and glycocalyx mediated contributions to cell adhesion identified by single cell force spectroscopy. Journal of physics Condensed matter : an Institute of Physics journal. 2010;22(19):194101.
114. Sabri S, Soler M, Foa C, Pierres A, Benoliel A, Bongrand P. Glycocalyx modulation is a physiological means of regulating cell adhesion. J Cell Sci. 2000;113 (Pt 9):1589-600.
115. Rozario T, DeSimone DW. The extracellular matrix in development and morphogenesis: a dynamic view. Developmental biology. 2010;341(1):126-40.
116. Frantz C, Stewart KM, Weaver VM. The extracellular matrix at a glance. J Cell Sci. 2010;123(24):4195-200.
117. Schaefer L, Schaefer RM. Proteoglycans: from structural compounds to signaling molecules. Cell Tissue Res. 2010;339(1):237-46.
118. Gordon MK, Hahn RA. Collagens. Cell Tissue Res. 2010;339(1):247-57.

119. Pankov R, Yamada KM. Fibronectin at a glance. J Cell Sci. 2002;115(Pt 20):3861-3.
120. Zollinger AJ, Smith ML. Fibronectin, the extracellular glue. Matrix biology : journal of the International Society for Matrix Biology. 2016.
121. Preissner KT. Structure and biological role of vitronectin. Annual review of cell biology. 1991;7:275-310.
122. Ruoslahti E. RGD and other recognition sequences for integrins. Annual review of cell and developmental biology. 1996;12:697-715.
123. Zhang WM, Kapyla J, Puranen JS, Knight CG, Tiger CF, Pentikainen OT, et al. alpha 11beta 1 integrin recognizes the GFOGER sequence in interstitial collagens. J Biol Chem. 2003;278(9):7270-7.
124. Massia SP, Rao SS, Hubbell JA. Covalently immobilized laminin peptide Tyr-Ile-Gly-Ser-Arg (YIGSR) supports cell spreading and co-localization of the 67-kilodalton laminin receptor with alpha-actinin and vinculin. J Biol Chem. 1993;268(11):8053-9.
125. Dee KC, Andersen TT, Bizios R. Design and function of novel osteoblast-adhesive peptides for chemical modification of biomaterials. Journal of biomedical materials research. 1998;40(3):371-7.
126. Arnold M, Cavalcanti-Adam EA, Glass R, Blummel J, Eck W, Kantlehner M, et al. Activation of integrin function by nanopatterned adhesive interfaces. Chemphyschem : a European journal of chemical physics and physical chemistry. 2004;5(3):383-8.
127. Wang X, Yan C, Ye K, He Y, Li Z, Ding J. Effect of RGD nanospacing on differentiation of stem cells. Biomaterials. 2013;34(12):2865-74.
128. Krebs HA. Chemical composition of blood plasma and serum. Annual review of biochemistry. 1950;19:409-30.
129. Wilson CJ, Clegg RE, Leavesley DI, Pearcy MJ. Mediation of biomaterial-cell interactions by adsorbed proteins: A review. Tissue Eng. 2005;11(1-2):1-18.
130. Sundin M, Ringden O, Sundberg B, Nava S, Gotherstrom C, Le Blanc K. No alloantibodies against mesenchymal stromal cells, but presence of anti-fetal calf serum antibodies, after transplantation in allogeneic hematopoietic stem cell recipients. Haematologica. 2007;92(9):1208-15.
131. Gstraunthaler G. Alternatives to the use of fetal bovine serum: serum-free cell culture. Altex. 2003;20(4):275-81.

132. Hayman EG, Pierschbacher MD, Suzuki S, Ruoslahti E. Vitronectin--a major cell attachment-promoting protein in fetal bovine serum. Experimental cell research. 1985;160(2):245-58.
133. Underwood PA, Bennett FA. A comparison of the biological activities of the cell-adhesive proteins vitronectin and fibronectin. J Cell Sci. 1989;93 (Pt 4):641-9.
134. Mazur P. Freezing of living cells: mechanisms and implications. The American journal of physiology. 1984;247(3 Pt 1):C125-42.
135. Baust JG, Gao DY, Baust JM. Cryopreservation An emerging paradigm change. Organogenesis. 2009;5(3):90-6.
136. Wang X, Hua TC, Sun DW, Liu BL, Yang GH, Cao YL. Cryopreservation of tissue-engineered dermal replacement in Me2SO: Toxicity study and effects of concentration and cooling rates on cell viability. Cryobiology. 2007;55(1):60-5.
137. Francois M, Copland IB, Yuan SL, Romieu-Mourez R, Waller EK, Galipeau J. Cryopreserved mesenchymal stromal cells display impaired immunosuppressive properties as a result of heat-shock response and impaired interferon-gamma licensing. Cytotherapy. 2012;14(2):147-52.
138. Janz FD, Debes AD, Cavaglieri RD, Duarte SA, Romao CM, Moron AF, et al. Evaluation of Distinct Freezing Methods and Cryoprotectants for Human Amniotic Fluid Stem Cells Cryopreservation. J Biomed Biotechnol. 2012.
139. de Menorval MA, Mir LM, Fernandez ML, Reigada R. Effects of Dimethyl Sulfoxide in Cholesterol-Containing Lipid Membranes: A Comparative Study of Experiments In Silico and with Cells. Plos One. 2012;7(7).
140. Galvao J, Davis B, Tilley M, Normando E, Duchen MR, Cordeiro MF. Unexpected low-dose toxicity of the universal solvent DMSO. Faseb J. 2014;28(3):1317-30.
141. Qi WD, Ding DL, Salvi RJ. Cytotoxic effects of dimethyl sulphoxide (DMSO) on cochlear organotypic cultures. Hearing Res. 2008;236(1-2):52-60.
142. Sasaki M, Kato Y, Yamada H, Terada S. Development of a novel serum-free freezing medium for mammalian cells using the silk protein sericin. Biotechnol Appl Bioc. 2005;42:183-8.
143. Brockbank KG, Heacox AE, Schenke-Layland K. Guidance for removal of fetal bovine serum from cryopreserved heart valve processing. Cells Tissues Organs. 2011;193(4):264-73.

144. Thirumala S, Wu X, Gimble JM, Devireddy RV. Evaluation of polyvinylpyrrolidone as a cryoprotectant for adipose tissue-derived adult stem cells. Tissue Eng Part C Methods. 2010;16(4):783-92.

145. Matsumura K, Hyon SH. Polyampholytes as low toxic efficient cryoprotective agents with antifreeze protein properties. Biomaterials. 2009;30(27):4842-9.

146. Kundu B, Kurland NE, Yadavalli VK, Kundu SC. Isolation and processing of silk proteins for biomedical applications. Int J Biol Macromol. 2014;70:70-7.

147. Chen FJ, Porter D, Vollrath F. Morphology and structure of silkworm cocoons. Mat Sci Eng C-Mater. 2012;32(4):772-8.

148. Aramwit P, Kanokpanont S, Nakpheng T, Srichana T. The Effect of Sericin from Various Extraction Methods on Cell Viability and Collagen Production. Int J Mol Sci. 2010;11(5):2200-11.

149. Terada S, Takada N, Itoh K, Saitoh T, Sasaki M, Yamada H. Silk Protein Sericin Improves Mammalian Cell Culture. In: Smith R, editor. Cell Technology for Cell Products. 3: Springer Netherlands; 2007. p. 397-401.

150. Zhaorigetu S, Yanaka N, Sasaki M, Watanabe H, Kato N. Silk protein, sericin, suppresses DMBA-TPA-induced mouse skin tumorigenesis by reducing oxidative stress, inflammatory responses and endogenous tumor promoter TNF-alpha. Oncol Rep. 2003;10(3):537-43.

151. Sasaki M, Kato N, Watanabe H, Yamada H. Silk protein, sericin, suppresses colon carcinogenesis induced by 1,2-dimethylhydrazine in mice. Oncol Rep. 2000;7(5):1049-52.

152. Cao Y, Wang B. Biodegradation of silk biomaterials. Int J Mol Sci. 2009;10(4):1514-24.

153. Miyamoto Y, Oishi K, Yukawa H, Noguchi H, Sasaki M, Iwata H, et al. Cryopreservation of Human Adipose Tissue-Derived Stem/Progenitor Cells Using the Silk Protein Sericin. Cell Transplant. 2012;21(2-3):617-22.

154. Toyosawa T, Oumi Y, Ogawa A, Sasaki M, Yamada H, Terada S. Novel Serum-Free Cryopreservation of Mammalian Cells Using Seric. In: Shirahata S, Ikura K, Nagao M, Ichikawa A, Teruya K, editors. Animal Cell Technology: Basic & Applied Aspects. Animal Cell Technology: Basic & Applied Aspects. 15: Springer Netherlands; 2009. p. 41-5.

155. Wu J, Rong Y, Wang Z, Zhou Y, Wang S, Zhao B. Isolation and characterisation of sericin antifreeze peptides and molecular dynamics modelling of their ice-binding interaction. Food Chem. 2015;174:621-9.
156. Livak KJ, Schmittgen TD. Analysis of relative gene expression data using real-time quantitative PCR and the 2(T)(-Delta Delta C) method. Methods. 2001;25(4):402-8.
157. Zamir E, Katz BZ, Aota S, Yamada KM, Geiger B, Kam Z. Molecular diversity of cell-matrix adhesions. J Cell Sci. 1999;112(11):1655-69.
158. Ruszova E, Cheel J, Pavek S, Moravcova M, Hermannova M, Matejkova I, et al. Epilobium angustifolium extract demonstrates multiple effects on dermal fibroblasts in vitro and skin photo-protection in vivo. Gen Physiol Biophys. 2013;32(3):347-59.
159. Huveneers S, Truong H, Faessler R, Sonnenberg A, Danen EHJ. Binding of soluble fibronectin to integrin alpha 5 beta 1 - link to focal adhesion redistribution and contractile shape. J Cell Sci. 2008;121(15):2452-62.
160. Memmo LM, McKeown-Longo P. The alpha v beta 5 integrin functions as an endocytic receptor for vitronectin. J Cell Sci. 1998;111:425-33.
161. Pang SP, Hernandez Y, Feng XL, Mullen K. Graphene as Transparent Electrode Material for Organic Electronics. Adv Mater. 2011;23(25):2779-95.
162. Pimenov SM, Ralchenko VG, Konov VI, Khomich A, Zavedeev EV, Frolov VD. Nanocrystalline diamond films - laser assisted fabrication, optical and electronic properties. Advanced Laser Technologies 2004. 2005;5850:230-41.
163. Verdanova M, Rezek B, Broz A, Ukraintsev E, Babchenko O, Artemenko A, et al. Nanocarbon Allotropes-Graphene and Nanocrystalline Diamond-Promote Cell Proliferation. Small. 2016;12(18):2499-509.
164. Martinez E, Engel E, Planell JA, Samitier J. Effects of artificial micro- and nano-structured surfaces on cell behaviour. Ann Anat. 2009;191(1):126-35.
165. Dolatshahi-Pirouz A, Jensen T, Kraft DC, Foss M, Kingshott P, Hansen JL, et al. Fibronectin adsorption, cell adhesion, and proliferation on nanostructured tantalum surfaces. Acs Nano. 2010;4(5):2874-82.
166. Baik KY, Choi J, Gwon H, Cho J, Kim YK, Attri P, et al. Adhesion and differentiation of human mesenchymal stem cells on plasma-functionalized graphenes with different feeding gases. Carbon. 2014;77:302-10.

167. Babchenko O, Kromka A, Hruska K, Kalbacova M, Broz A, Vanecek M. Fabrication of nano-structured diamond films for SAOS-2 cell cultivation. Phys Status Solidi A. 2009;206(9):2033-7.

168. Higgins AM, Banik BL, Brown JL. Nanotopography Sensing Through Intracellular Signaling and Mechanotransduction with an Emphasis on Bone. J Biomater Tiss Eng. 2013;3(4):396-408.

169. Curtis ASG, Dalby M, Gadegaard N. Cell signaling arising from nanotopography: implications for nanomedical devices. Nanomedicine-Uk. 2006;1(1):67-72.

170. Sousa SR, Moradas-Ferreira P, Barbosa MA. TiO2 type influences fibronectin adsorption. J Mater Sci-Mater M. 2005;16(12):1173-8.

171. Dekker A, Reitsma K, Beugeling T, Bantjes A, Feijen J, Vanaken WG. Adhesion of Endothelial-Cells and Adsorption of Serum-Proteins on Gas Plasma-Treated Polytetrafluoroethylene. Biomaterials. 1991;12(2):130-8.

172. Campillo-Fernandez AJ, Unger RE, Peters K, Halstenberg S, Santos M, Sanchez MS, et al. Analysis of the Biological Response of Endothelial and Fibroblast Cells Cultured on Synthetic Scaffolds with Various Hydrophilic/Hydrophobic Ratios: Influence of Fibronectin Adsorption and Conformation. Tissue Eng Pt A. 2009;15(6):1331-41.

173. Iwamoto GK, Winterton LC, Stoker RS, Vanwagenen RA, Andrade JD, Mosher DF. Fibronectin Adsorption Detected by Interfacial Fluorescence. J Colloid Interf Sci. 1985;106(2):459-64.

174. Hayman EG, Pierschbacher MD, Ohgren Y, Ruoslahti E. Vitronectin (Serum Spreading Factor) Is Present at the Cell-Surface and in Tissues. J Cell Biol. 1983;97(5):A96-A.

175. Carre A, Lacarriere V. How Substrate Properties Control Cell Adhesion. A Physical-Chemical Approach. J Adhes Sci Technol. 2010;24(5):815-30.

176. Audiffred JF, De Leo SE, Brown PK, Hale-Donze H, Monroe WT. Characterization and Applications of Serum-Free Induced Adhesion in Jurkat Suspension Cells. Biotechnol Bioeng. 2010;106(5):784-93.

177. Shen Y, Jacobs JM, Camp DG, 2nd, Fang R, Moore RJ, Smith RD, et al. Ultra-high-efficiency strong cation exchange LC/RPLC/MS/MS for high dynamic range characterization of the human plasma proteome. Anal Chem. 2004;76(4):1134-44.

178. Kim YL, Im YJ, Lee YK, Ha NC, Bae YS, Lim SM, et al. Albumin functions as an inhibitor of T cell adhesion in vitro. Biochem Biophys Res Commun. 2006;351(4):953-7.
179. Rezek B, Kratka M, Kromka A, Kalbacova M. Effects of protein inter-layers on cell-diamond FET characteristics. Biosensors & bioelectronics. 2010;26(4):1307-12.
180. Rodan SB, Imai Y, Thiede MA, Wesolowski G, Thompson D, Barshavit Z, et al. Characterization of a Human Osteosarcoma Cell-Line (Saos-2) with Osteoblastic Properties. Cancer Res. 1987;47(18):4961-6.
181. Pautke C, Schieker M, Tischer T, Kolk A, Neth P, Mutschler W, et al. Characterization of osteosarcoma cell lines MG-63, Saos-2 and U-2 OS in comparison to human osteoblasts. Anticancer research. 2004;24(6):3743-8.
182. Humphries MJ, Akiyama SK, Komoriya A, Olden K, Yamada KM. Identification of an alternatively spliced site in human plasma fibronectin that mediates cell type-specific adhesion. J Cell Biol. 1986;103(6 Pt 2):2637-47.
183. Mager MD, LaPointe V, Stevens MM. Exploring and exploiting chemistry at the cell surface. Nat Chem. 2011;3(8):582-9.
184. Khalili AA, Ahmad MR. A Review of Cell Adhesion Studies for Biomedical and Biological Applications. Int J Mol Sci. 2015;16(8):18149-84.
185. Saoncella S, Echtermeyer F, Denhez F, Nowlen JK, Mosher DF, Robinson SD, et al. Syndecan-4 signals cooperatively with integrins in a Rho-dependent manner in the assembly of focal adhesions and actin stress fibers. Proc Natl Acad Sci U S A. 1999;96(6):2805-10.
186. Chen RH, Sarnecki C, Blenis J. Nuclear localization and regulation of erk- and rsk-encoded protein kinases. Molecular and cellular biology. 1992;12(3):915-27.
187. Baust JM, Van Buskirk R, Baust JG. Modulation of the cryopreservation cap: elevated survival with reduced dimethyl sulfoxide concentration. Cryobiology. 2002;45(2):97-108.
188. Toyosawa T, Oumi Y, Ogawa A, Sasaki M, Yamada H, Terada S. Novel Serum-Free Cryopreservation of Mammalian Cells Using Sericin. Anima Cell Tech. 2009;15:41-5.
189. Ohnishi K, Murakami M, Morikawa M, Yamaguchi A. Effect of the silk protein sericin on cryopreserved rat islets. J Hepato-Bil-Pan Sci. 2012;19(4):354-60.